Ecole Polytechnique
Fédérale de Lausanne

Urban Thermodynamics

Project :
Urban overheating mitigation strategies for EPFL Innovation Park

Authors

Alexandre Delgado, SCIPER : 339723
Edouard Thoumas, SCIPER : 362532
Romain Fastenaekels, SCIPER : 355620
Lucien Othenin-Girard, SCIPER : 346201
Bastien Fuhrer, SCIPER : 341051

Group 3

8 janvier 2025

Assist. Prof. Dolaana Khovalyg

CIVIL-309
Fall - 2024

Table of contents

1 Introduction

The persistent development of urban regions presents expanding challenges for the environment and the quality of life of their inhabitants. Changes in urban density, morphology, and construction materials, together with the escalated of human exercises, produce critical natural impacts. Among these impacts, the Urban Heat Island (UHI) effect is one of the most prominent : temperature in urban areas are often higher than in surrounding regions, particularly during heat waves. This phenomenon, combined with global climate change, can have serious consequences, affecting human health through increased thermal discomfort, morbidity, and heat-related mortality, as well as driving up energy demand.

In this context, studying the urban microclimate becomes essential. Understanding how urban elements influence thermal dynamics and energy exchanges within a city can offer solutions to mitigate UHI. This project focuses precisely on this topic : it aims to analyze the influence of various urban elements on the microclimate and explore strategies to mitigate urban warming at the EPFL Innovation Park, a site representative of the diversity of materials and contemporary urban configurations. Located near Lake Leman, this site integrates various surface materials(asphalt, sandy soil, concrete...) and a range of structures and green spaces.

The project is structured around three main objectives :

1. Analyzing the current conditions of the site in relation to its microclimate, taking into account its climatic and morphological characteristics as well as the vegetation and materials present.
2. Studying the individual effects of buildings, ground surfaces, vegetation, and water on the urban microclimate to understand their specific contributions to the local microclimate.
3. Proposing integrated mitigation solutions combining several urban elements to optimize thermal exchanges and improve thermal comfort within the study area.

We will rely on the use of a microclimate simulation model, ENVI-met, which will allow us to simulate future scenarios based on the RCP 8.5 climate pathway projected for the year 2100. Through this approach, we aim not only to assess the impacts of urban elements on the local climate but also to propose solutions based on climate-responsive design principles to promote more resilient and sustainable urban development.

The report structure will follow these objectives : the first section will analyse the site's conditions, the second will explore microclimatic interactions, and the final section will propose suitable mitigation strategies. Based on rigourous analyses and detailed simulations, this report aims to provide concrete guidance for climate-conscious urban planning that promotes public health and sustainability.

2 Site analysis

2.1 EPFL Innovation Park (presentation)

The EPFL Innovation Park is a dynamic campus dedicated to innovation and research, situated, as we stated before, on the Ecole Polytechnique Fédérale de Lausanne (EPFL) campus near Lac Léman. This site is home to a variety of buildings that host research laboratories, startups, and established companies, making it a hub of scientific and technological activity. The park's layout integrates a complex network of roads and pedestrian pathways, allowing us to move around quite easily. The architectural diversity, including glass, concrete, and metal facades of various heights, contributes to the unique character of the site, influencing factors such as shading, solar reflection, and wind patterns. The road network and surface materials like asphalt, concrete, grass, and gravel create varied thermal properties, impacting how heat is absorbed, stored, and released throughout the day. Additionally, green spaces and landscaping are interwoven within the built environment, offering potential cooling effects but also interacting with the surrounding structures and ground surfaces in ways that shape the local microclimate.

2.2 Visite site

To study the elements influencing the microclimate of this site, an on-site visit was organized on October 14, allowing for direct exploration of the urban and microclimatic characteristics of the park. Following a specific route connecting locations from A to G, we recorded various data points at each observation site, including building heights, construction materials, vegetation, and potential sources of anthropogenic heat.

During this exploration, we used direct observation methods and simple tools, such as fisheye camera application to estimate the sky view factor, which allowed us to quantify the visible sky portion at each location. this estimation is essential to understand the direct sunlight exposure and natural cooling potential of the site. Additionally, we took into account the road network, ground cover materials, and shading sources to better identify zones susceptible to summer overheating.

The tables below summarize the collected data, divided into three parts for better readability. Table 1 highlights the natural elements and ground cover materials at each location. Table 2 provides information on the surrounding building materials and their heights. Finally, Table 3 presents anthropogenic heat sources, aspect ratios, sky view factors, and shading sources for each observed location. This structured presentation offers a clear overview of the characteristics influencing the microclimate within the park and will serve as a basis for further analysis and simulation.

Location	Natural Elements	Ground Cover Material
A	Trees, small shrubs	Asphalt
B	Gardens	Concrete, grass
C	Trees, landscaping	Grass, gravel
D	Few trees, grass	Asphalt, tiles
E	Trees, bushes, plants	Concrete, small gardens
F	Minimal vegetation	Asphalt, concrete
G	Trees, small plants	Concrete, grass

TABLE 1 – Site Analysis - Part 1 : Natural Elements and Ground Cover Material

I don't think all the buildings there have the same number of stories.

Location	Surrounding Building Material	Building Height
A	Glass, concrete, aluminium	3-4 stories
B	Concrete, steel, aluminium, glass	3-4 stories
C	concrete, aluminium	3-4 stories
D	Glass, steel, wood, PVC	3-4 stories
E	Glass, concrete, steel	3-4 stories
F	Concrete, steel, glass	3-4 stories
G	Glass, concrete	3-4 stories

TABLE 2 – Site Analysis - Part 2 : Surrounding Building Material and Building Height

These observations will be used as input data in the ENVI-met software to simulate the current microclimatic conditions of the site. Using ENVI-met, we will evaluate how different urban and natural characteristics influence surface temperatures, relative humidity, and air circulation. This simulation approach will allow us to visualize the effects of the park's elements on the microclimate and test mitigation scenarios to optimize thermal comfort and reduce urban heat island effects.

Location	Anthropogenic Heat Source	Aspect Ratio	Sky View Factor	Shading Sources
A	Vehicles	1 :3	High (90-100%)	/
B	Vehicle exhaust, AC units	1 :2	High (70-80%)	Buildings, Plants
C	AC units	1 :3	High (90-100%)	Buildings, trees
D	Office equipment	1 :3	High (80-90%)	Buildings, trees
E	Parking heat, vehicles	1 :3	High (70-80%)	Buildings, trees
F	Industrial sources, vehicles	1 :3	High (80-90%)	Buildings
G	Machinery, heating systems	1 :3	High (80-90%)	Trees, buildings

TABLE 3 – Site Analysis - Part 3 : Anthropogenic Heat Source, Aspect Ratio, Sky View Factor, and Shading Sources

2.3 Launching of ENVI-met

2.3.1 Definition of Materials

The first step in setting up the ENVI-met simulation is to prepare the materials representing building facades and roofs, as they play a crucial role in defining the site's thermal dynamics. Accurate material definitions allow the model to simulate how each surface absorbs, stores, and releases heat, which is essential for assessing the Urban Heat Island effect and understanding the impact of construction materials on the local microclimate.

This preparation is done through the Database Manager tool in ENVI-met, where we input detailed thermal and physical properties for each observed material. For this project, we used the Ubakus tool to obtain reliable values for properties like thickness or specific heat capacity, ensuring the materials are well-represented in the simulation.
However, we did not have access to the transmissivity, emissivity, and absorption properties for each material, so we relied on other sources for these parameters.

For the building materials, we referred to the table provided in figure 51 of the appendix, which categorizes the facade and roof components of three building groups (A, B, and C) with detailed descriptions of each layer's material and thickness. This table served as a reference to input accurate material characteristics into ENVI-met, ensuring that the thermal properties of each building are represented as observed on-site.
Furthermore, the map in Appendix 52 provides a visual representation of the EPFL Innovation Park, highlighting the locations of the different building groups to situate them within the overall site layout.

To address the issue that ENVI-met allows only three layers per material, we had to adapt the thermal properties for cases where four layers were present. Specifically, we combined the thermal conductivities of the XPS and gravel layers into a single equivalent conductivity using the following formula :

$$\frac{1}{K_{\text{combined}}} = \frac{L_1}{k_1} + \frac{L_2}{k_2} \tag{1}$$

For the values of reflectivity, absorption, and emissivity, we used those of the outermost layer, as it has the greatest influence on surface interactions with the environment.
For other properties, such as specific heat capacity and density, we applied a thickness-weighted average using the following formula :

$$\text{Property}_{\text{average}} = \frac{\sum_{i\in\{\text{XPS, Gravel}\}}(\text{Property}_i \times L_i)}{\sum_{i\in\{\text{XPS, Gravel}\}} L_i} \tag{2}$$

These adjustments ensured that the material properties input into ENVI-met are representative of the physical behavior of the multi-layered construction materials, despite the software's limitations.
The values obtained for the two combined layers are provided in Appendix fig. 54.

2.3.2 Preparation of the real case simulation

After defining the materials, the next step involves using the "Space" module in ENVI-met to set up the simulation environment. In this step, we upload a map of the site to serve as the base layout for the simulation. Using this map, we introduce the key elements required for the simulation, including the distribution of building materials, vegetation, and soil types.
For vegetation, we primarily placed trees, ensuring their positions and characteristics matched the real layout. For the soil, we assigned the predefined types based on the observed conditions on-site (according to Appendix fig. 53). These elements were carefully distributed across the map to reflect the actual layout of the EPFL Innovation Park, ensuring that the simulation accurately represents the site's microclimatic conditions.
Now, we shift our focus to analyzing the real-case scenario. For this analysis, we positioned ourselves at the pedestrian level ($k = 5$, corresponding to a height of 1.5 m) as it represents the height most relevant to thermal comfort experienced by individuals. This approach allows us to evaluate how water bodies and urban configurations influence the microclimate directly at the level where people interact with their environment, ensuring a more accurate assessment of the practical implications for urban thermal comfort.

2.4 Analysis of the real-case simulation

2.4.1 Weather file

A brief analysis of the climate condition is nice, but it can be improved by considering other environmental parameters and be used to set direction for your intervention.

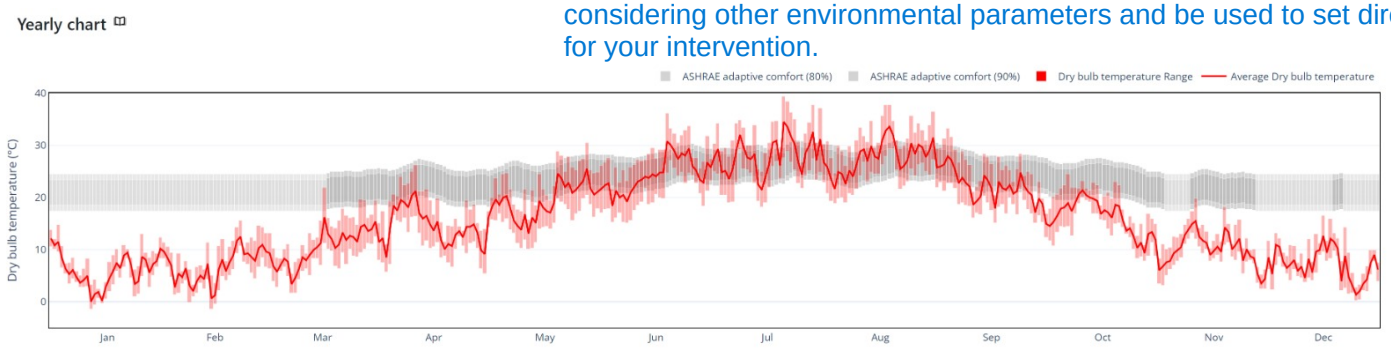

FIGURE 1 – Dry Bulb Temperature during the year

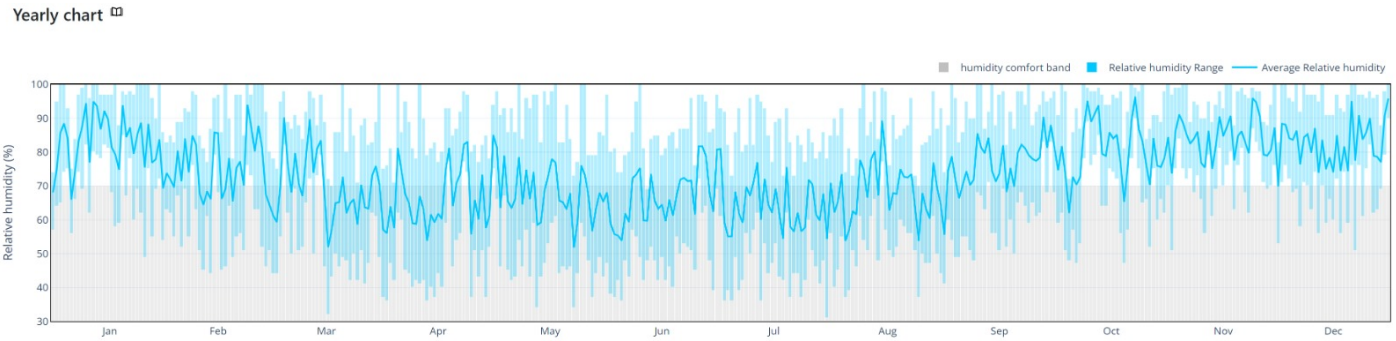

FIGURE 2 – Relative humidity during the year

We uploaded the EPW weather file to the CBE Tool provided by UC Berkeley to analyze the local climate conditions. The tool generated two charts for our analysis.

Fig. 1 illustrates the dry bulb temperature over the course of the year. The red line represents the average dry bulb temperature, while the shaded grey area indicates the comfort range based on ASHRAE adaptive comfort standards. From this figure, it is evident that temperatures peak during the summer months, particularly from late June to August, where the average temperatures consistently rise above

the comfort range.

Fig. 2 shows the relative humidity variation throughout the year. The blue line represents the average relative humidity, while the shaded area highlights the acceptable comfort band for humidity. During the summer months, the relative humidity appears slightly lower compared to other times of the year, which coincides with the higher temperatures observed in fig. 1.

From these observations, the hottest months are identified as July and August, where temperatures reach their peak and relative humidity is lower, creating a distinct summer climate profile. For our simulations, we specifically based our parameters on the conditions recorded on August 18th.

2.4.2 Wind Dynamics

Although extensive presentation of the simulation results of current site, local critical locations and parameters are not identified. Lacking depth of analysis. There is no outdoor thermal comfort analysis.

The influence of buildings on urban wind dynamics plays a critical role in understanding how urban morphology affects microclimatic comfort. The ENVI-met simulation revealed that buildings significantly modify wind patterns by creating zones of turbulence and calm. At lower levels, the presence of buildings increases surface roughness, which reduces wind speed. This effect is more pronounced in areas with higher building density and taller structures.

The simulation also highlighted the three-dimensional nature of airflow in urban environments. Buildings generate turbulence and air recirculation zones, causing sudden changes in wind direction and speed. These variations are particularly noticeable in specific areas where airflow is disrupted, as shown in the wind speed map below. Additionally, narrow streets act as channels that amplify longitudinal wind speeds, creating a tunnel effect. This phenomenon is especially visible in the northern part of the Innovation Park, where the wind accelerates in confined spaces while adjacent areas remain more sheltered.

These findings underscore the complexity of urban wind dynamics and their implications for pedestrian comfort and the design of public spaces. The provided wind speed visualization effectively illustrates these interactions, emphasizing the need to account for such factors in urban planning. If unaddressed, these dynamics could exacerbate discomfort in outdoor spaces or disrupt intended uses.

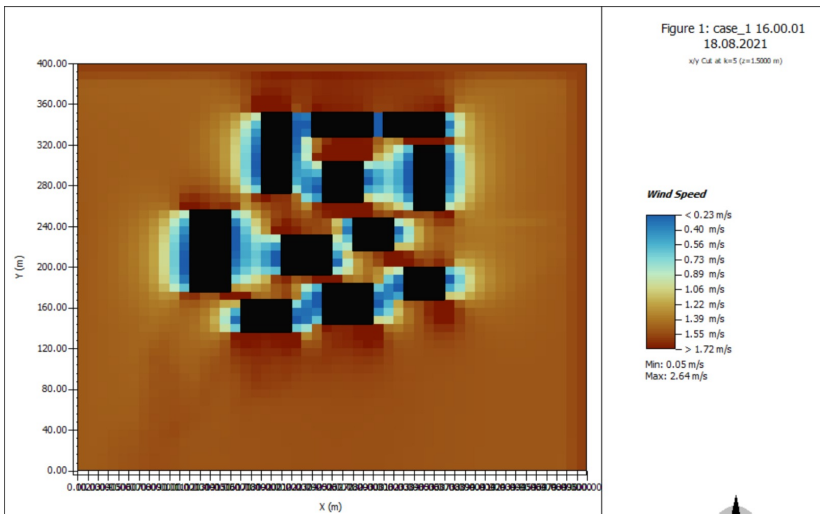

FIGURE 3 – Basic case Wind Speed

2.4.3 Analysis of the Relative Humidity

Relative humidity is influenced not only by vegetation but also by the interaction between air temperature and building materials. As the air temperature increases, its capacity to hold water vapor rises, which can reduce relative humidity unless additional moisture is introduced into the environment. This is evident in the southern area of the Innovation Park, where vegetation mitigates air temperature through

shading and evapotranspiration, maintaining higher relative humidity levels compared to exposed areas.

Building materials also play a significant role in regulating humidity levels. Surfaces with higher thermal inertia, such as asphalt or concrete, retain heat and reduce the likelihood of evaporation, leading to lower relative humidity. In contrast, permeable or vegetated surfaces enable water exchange, adding moisture to the air. These differences are reflected in the maps, where the areas with dense vegetation and cooler air temperatures align with higher relative humidity, while the warmer zones with impermeable surfaces show reduced humidity.

The interplay between air temperature and relative humidity, as well as the role of material properties, highlights the importance of integrating vegetation and thoughtful material selection in urban design. These elements not only improve thermal comfort but also stabilize humidity levels, creating more balanced and livable microclimates.

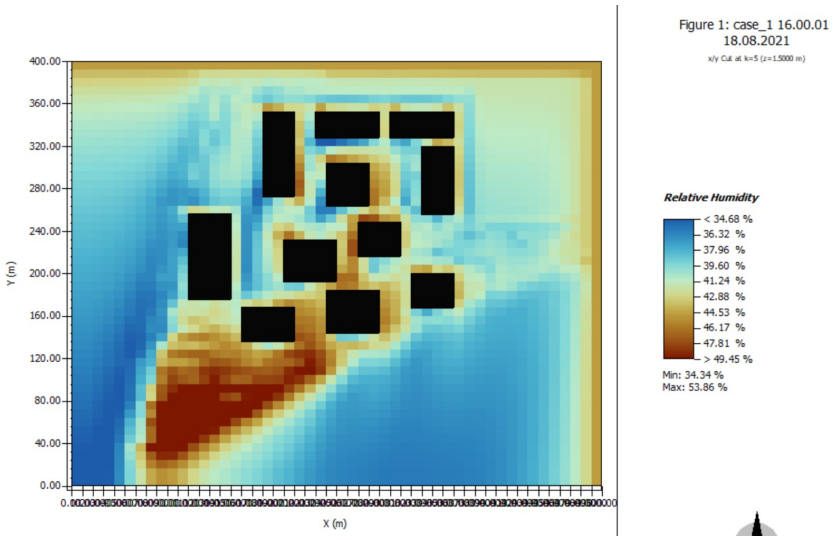

FIGURE 4 – Basic case Relative humidity

2.4.4 Effects of Vegetation and Buildings on Urban Temperature and Radiation Dynamics

The images below provide a clear representation of the relationship between soil temperature and direct solar radiation, highlighting the cooling effects of both vegetation and buildings. The soil temperature map shows that areas with dense vegetation experience significantly lower temperatures. This cooling effect is due to the dual action of vegetation : shading and evapotranspiration. Trees and plants intercept solar radiation, reducing the amount of energy that reaches the ground. Simultaneously, they release moisture into the air through evapotranspiration, which consumes energy and lowers the surrounding temperature.

The direct radiation map further illustrates the impact of shading, particularly from buildings. Tall structures create zones of reduced solar exposure, with shadows varying in intensity based on the height, orientation, and spacing of the buildings. These shaded areas directly correspond to cooler soil temperatures in the temperature map. Additionally, the materials and colors of building facades influence the extent of heat mitigation, as reflective surfaces reduce the absorption of solar radiation, helping to maintain lower temperatures in shaded zones. Precast concrete walls, especially those in lighter colors, can significantly reflect sunlight, thus reducing heat accumulation. Similarly, plastered surfaces painted in white or other light shades enhance this reflective quality, contributing to a cooler environment. Fiber cement panels, chosen for their durability, also aid in temperature regulation when finished with reflective coatings.

The maps together highlight the contrasting effects of exposed and shaded surfaces. Areas with minimal vegetation or building coverage show higher temperatures due to the direct absorption of radiation by impermeable surfaces like asphalt or concrete. These materials retain and release heat slowly, contributing

to the urban heat island effect. In contrast, zones with a combination of vegetation and building shade demonstrate the most significant cooling, emphasizing the synergistic effect of natural and built features.

Thus, strategic placement of green spaces and carefully oriented buildings can significantly reduce radiation and ground temperatures, enhancing thermal comfort and mitigating heat stress in urban environments. The maps visually reinforce these conclusions, showing how these elements interact to shape the local microclimate effectively.

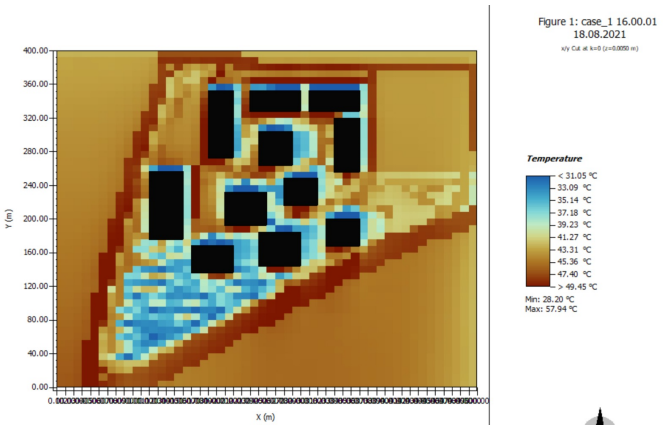

FIGURE 5 – Basic case soil temperature

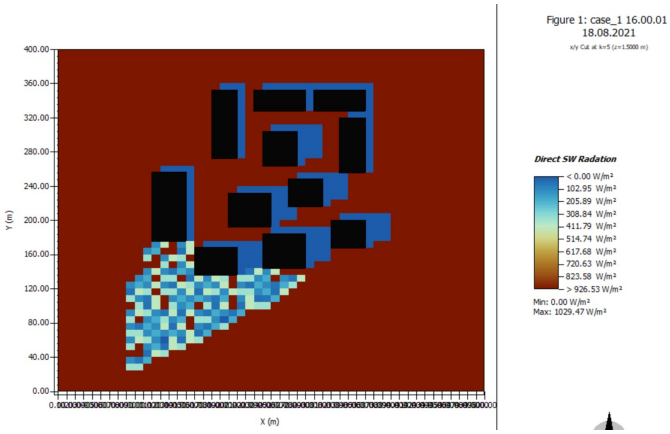

FIGURE 6 – Basic case Radiation

As we can see below, air temperature and ground temperature have similar causes, but air temperature is also influenced by the wind, which can create corridors of cool or warm air.

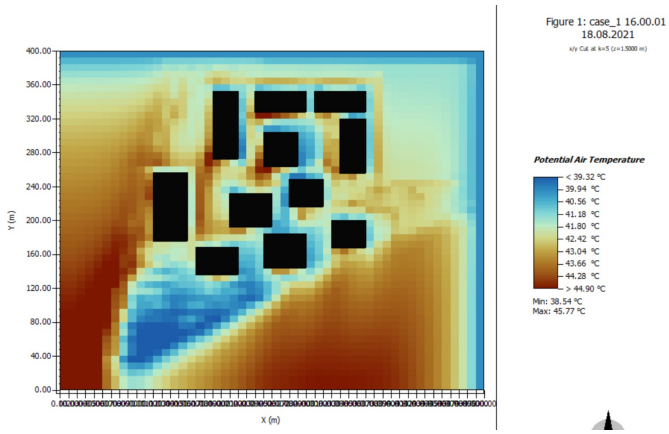

FIGURE 7 – Basic case potential air temperature

3 Urban microclimate exploration

In this section, we will explore how different urban elements influence the microclimate by modifying the real-case simulation. To achieve this, we will conduct comparative analyses by running two simulations for each type of interaction. These simulations are designed to isolate and analyze the effects of individual elements —buildings, ground surfaces, vegetation, and water bodies— on the urban microclimate. For each interaction, one element is modified to better analyze its effect, while all other changes are implemented with the aim of improving the local microclimate. By comparing the results, we aim to better understand the specific contributions of each element and identify strategies to optimize thermal comfort and mitigate the Urban Heat Island effect.

3.1 Building-environment interactions

3.1.1 Modifications

An explanation of the rationale of the modifications is needed.

In this part, we are going to analyse two different scenarios regarding building morphology. The changes that we made from the base case were the following.

— **Case A** : The buildings all have the same height (12m). However, we chose the buildings' width to have the smallest distance possible between them. Furthermore, we added green walls and green roofs by selecting the item "green + sandyloam" for both roofs and walls in ENVI-MET.

— **Case B** : This time, the buildings are higher and thinner. They still all have the same height (25m), but here, the width maximizes the distance between the buildings. We didn't add any green walls.

3.1.2 Results : Air temperature

Why is air temperature delta used instead of potential air temperature?

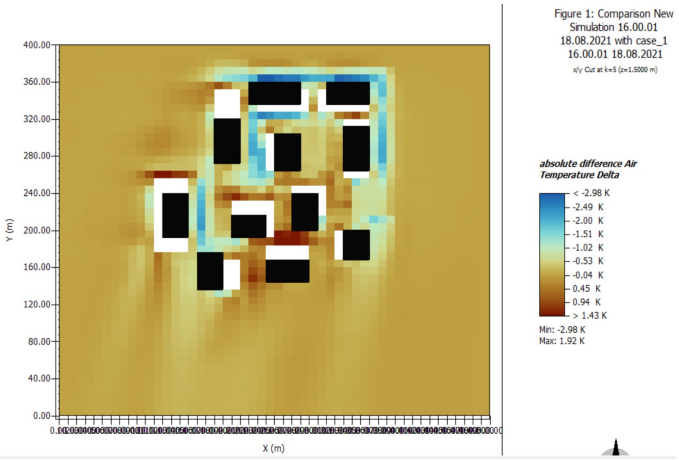

FIGURE 8 – Air temperature difference between basic case and case B at 4pm

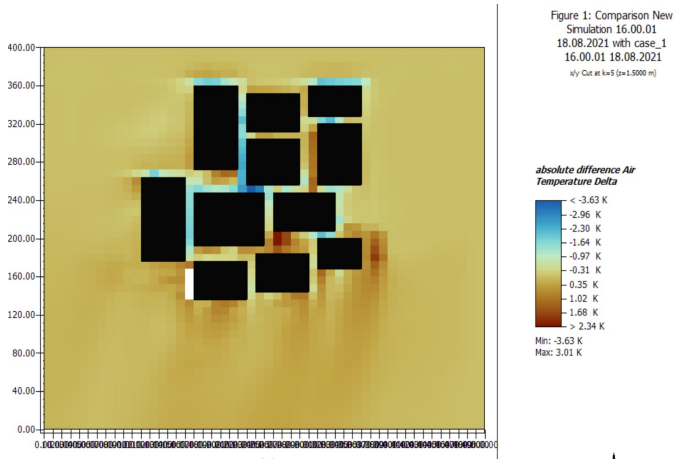

FIGURE 9 – Air temperature difference between basic case and case A at 4pm

The potential air temperature is the first parameter we will analyse. The results are shown in Figure 8 and Figure 9. For the case A, the buildings are now closer to each other, which means that the narrow streets have a lot of shading. As we can see in fig. 9, most of the time the air temperature drops between buildings which was expected. As for the second case, the buildings are now much taller and therefore provide a lot of shading. Here, the air temperature drops again but tends to do it in the middle of the street and not close to the building. This can be explained by the fact that the fig. 8 shows the difference in air temperature between the case B and the basic case. In the basic case, the buildings are shorter and the middle of the streets is more exposed to sun irradiance. This is why we cans see a much lower air temperature in the second case. We can also see that the two top buildings have been moved up and as a result, the air temperature just above them dropped down. From the figure, we can estimate that the sun irradiance was coming from the south-west.

3.1.3 Results : wind speed and direction

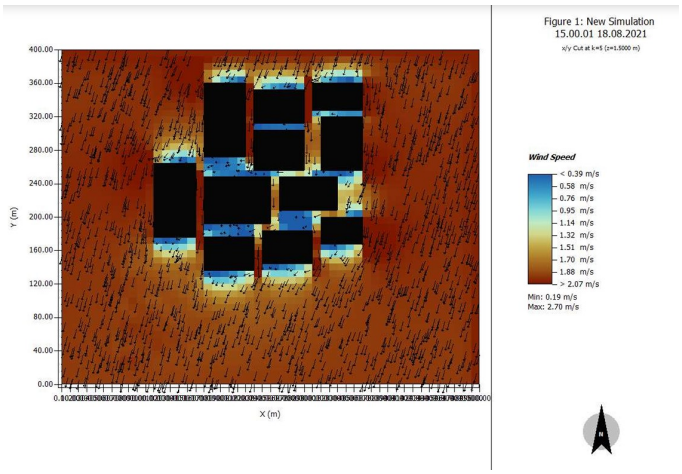

FIGURE 10 – Wind for case A at 3pm

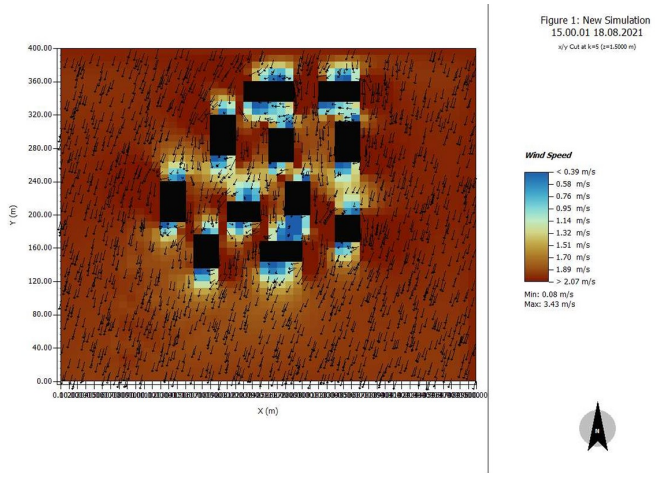

FIGURE 11 – Wind for case B at 3pm

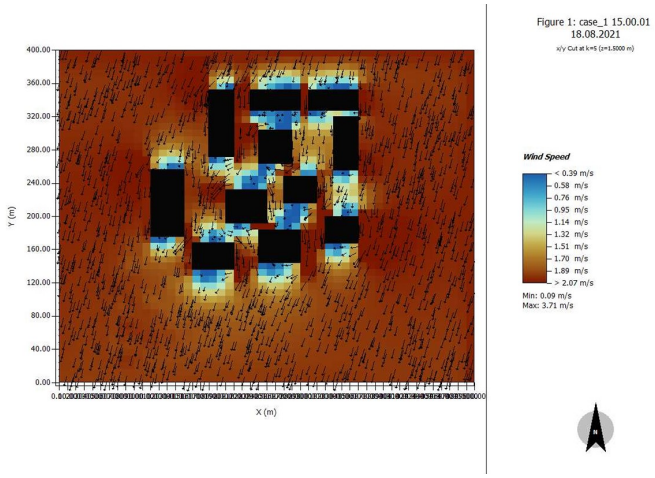

FIGURE 12 – Wind for basic case at 3pm

If the wind direction is perpendicular to the building axis, it will have less tendency to enter the streets and will tend to "jump" from roof to roof. Therefore, less vortices will appear in the street canyon. If the wind direction is parallel to the building axis, the street canyon will provide an optimal space for the wind to blow. This phenomenon is known as channelling. If the wind direction is neither perpendicular nor parallel, a combination of the two cases will develop. The wind will partly skip above the canyon and partly enter it, moving in a helical flow.

In case A, the buildings are very close to each other and as expected the maximal wind speed is the lowest of all cases. This due to the fact that the wind skips from building to building without entering the streets. Between the buildings, the wind speed even slows down to nearly 0 m/s. We can also see that when the streets are oriented according to the wind direction this causes channelling and the wind speed is much higher.

In case B, the buildings are more spaced out and the wind can enter the streets. The maximal wind speed is now greater than in case A. The placement of the buildings is also very important, for example in figure11 we can see that the vertical streets provide a straight line for the wind to go through (channelling). We can also see that the buildings that are aligned with each other create a low speed wind line.

For both cases, we can see that the wind direction changes when it approaches a building. Most of it go around the buildings but part of the wind is stuck in the middle. This corresponds to the stagnation

point of the building surface. The same behaviour can usually be observed when studying wind flow on the vertical axis : the wind can go over the building, but if its position corresponds to the stagnation point, the wind speed will be zero.

What about the associated change in radiant temperature?

3.2 Ground-environment interactions

In this part we are going to change different surfaces of the ground. The goal is to have less heat islands and lower temperature in general. The materials can have different behaviors with respect to their reflectivity and permeability. The main places where we have high temperature are on parking and roads.

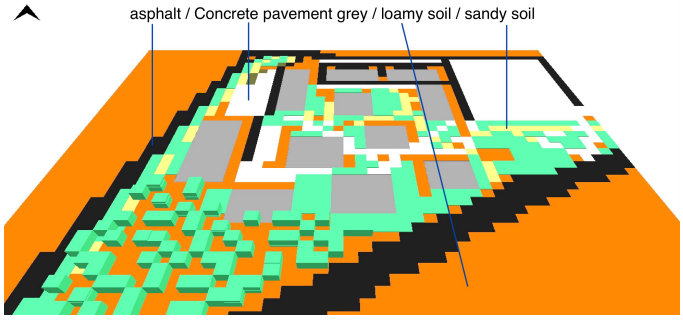

FIGURE 13 – Basic case ground

3.2.1 Modifications

A better explanation of the choice of material, linking to thermal behaviours and energy exchange processes is needed.

In scenario 1, we decided to change the ground of the parking with yellow bricks and for the small paths made of unsealed (loam) soil. We also changed the asphalt with red asphalt which should give us better results. We applied the solution only on the top part of the road as the bottom and left one have a higher traffic which requires a better material such as normal asphalt. In the scenario 2, red bricks will replace the concrete in parking and light concrete pavement is going to take the place of the asphalt. The modifications can be observed more precisely on figure 14 and 15

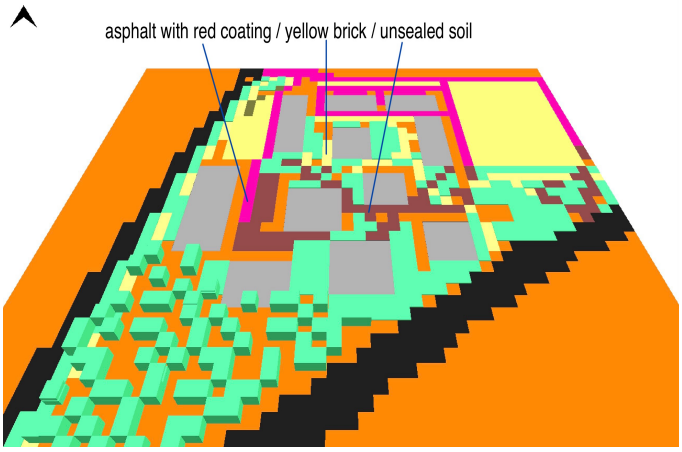

FIGURE 14 – Variation A

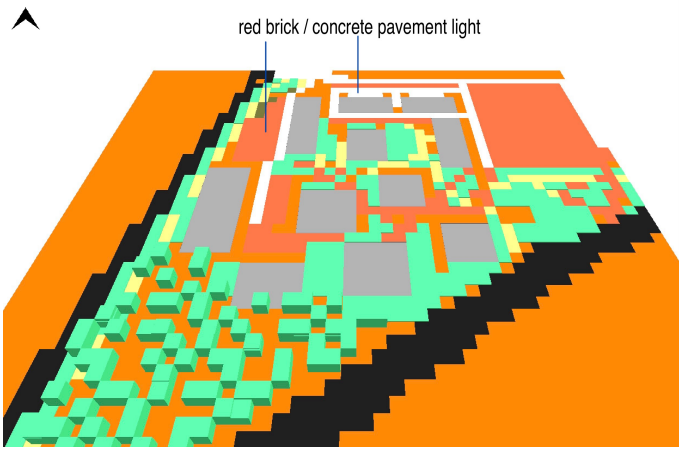

FIGURE 15 – Variation B

3.2.2 Comparison of the two scenarios

Why use a relative term instead of absolute value?

The first parameter we will analyze is the surface temperature right at the ground level. The obtained results are shown in Figure 16 and 17. The two maps consist of comparing the surface temperature of variation 1 minus the one of variation 2 in relative percentage with respect to variation 2 : (Variation 1 - Variation 2)/Variation 2. The figure on the left shows the difference at 7 am while the one on the right is at 3 pm.

We can immediately see a huge performance up to 20% due to the use of unsealed soil in the afternoon compared to the red brick. We can see the advantage of plotting the result in the morning too as it is observable that the unsealed soil has actually a higher temperature up to +6% at 7 am. The results suggest that bricks have a higher variation between the day and the night compared to unsealed soil which seems less affected by the radiation. It aligns with the difference in terms of evaporation between the two, unsealed soil having its thermal behavior heavily influenced by moisture content and evapotranspiration.

The yellow brick constantly has a temperature between -6 and -10% compared to red ones which indicates a better solution is to use yellow ones. This result corresponds to what we were expecting as yellow brick has a lower albedo. They reflect more solar radiation leading to lower surface temperature. The light concrete pavement seems a bit more efficient during the morning (only around -1%) but loses its advantage during the afternoon reaching around +3% compared to red asphalt.

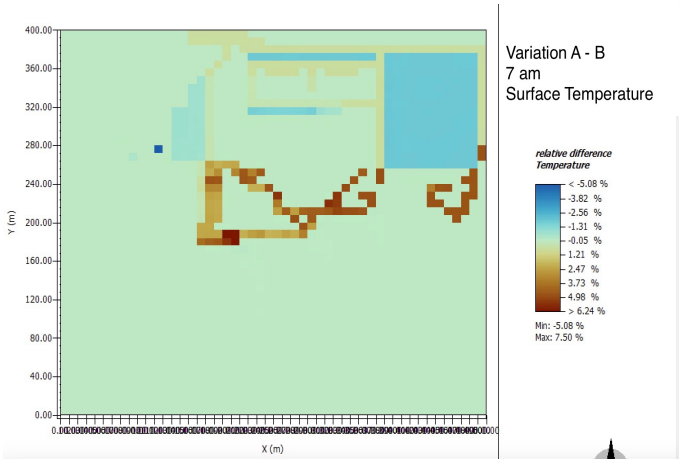

FIGURE 16 – ground surface temperature difference at 7 am

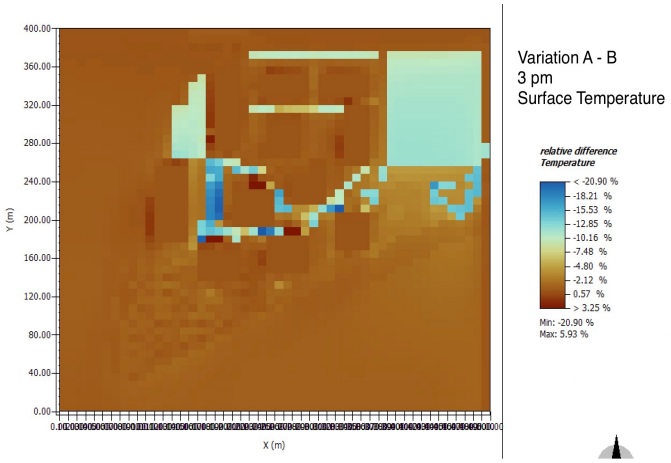

FIGURE 17 – ground surface temperature difference at 3 pm

The Figure 18 represents the same difference but in air temperature at 1.5 m elevation at 3 pm compared to the surface temperature we analyzed before. It is useful to look at the air temperature and not only the ground if we want to check if the variation also has an impact at the human height and in which direction we will feel a bigger impact. The figure shows that the effect on the air temperature is bigger from the parking than from the roads. That observation is normal because parking have a bigger area compared to narrower paths and thus can have a bigger vertical mixing with the air temperature. We can also clearly observe the wind being directed North-South which means that an amelioration at the top of the map would have a bigger effect than one at the bottom.

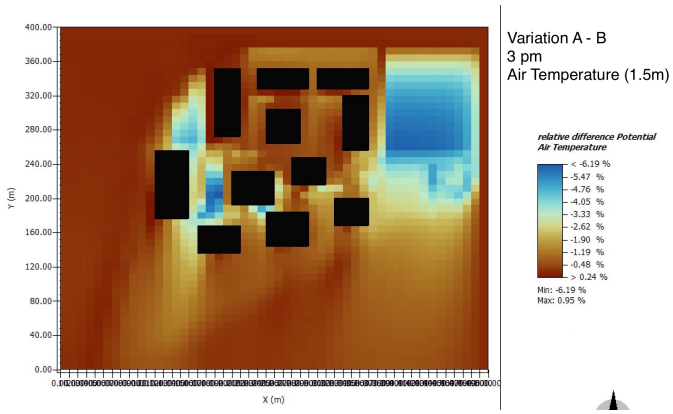

FIGURE 18 – Ground air temperature difference at 3 pm

3.2.3 Comparison with the basic case

We will now compare the variation A with the basic case as the 3 previous figure show us that this variation is better for the temperature. The Figures 19 and 20 represent the difference of surface temperature and air temperature at 3 pm by doing : (temperature A - temperature base)/ temperature base.
We can observe as we could imagine that red asphalt is way better than the classic version (up to -15%). It is a result we could think about from the start since asphalt is a really bad material in terms of temperature and UHI effect. Something we were not expecting on the other hand is the unsealed soil being worse than the concrete pavement. For some areas, the difference increases by 10% with the unsealed soil, which is something we want to avoid. The yellow brick seems to be equivalent to concrete pavement since no difference is clearly detected. And we can conclude that the basic case is actually a great solution. The only point on which we could work is the utilization of a red coating for the asphalt. The Figure 20 in particular confirms what we said previously. There's no huge benefits observable from the variation we made except for the red coating. The effect as mentioned above looks more significant from the vertical modified roads than for the horizontal ones. That confirms the idea that effects obtained at the northern part of the map are transported downstream due to the wind. That would motivate us to apply a red coating on all the top and left part of asphalt as it could have a huge impact on the bottom part. We would also apply the red coating on the horizontal roads at the top since the reduction of the surface temperature around -15% is significant even if the impact would be smaller than the one of the vertical roads.

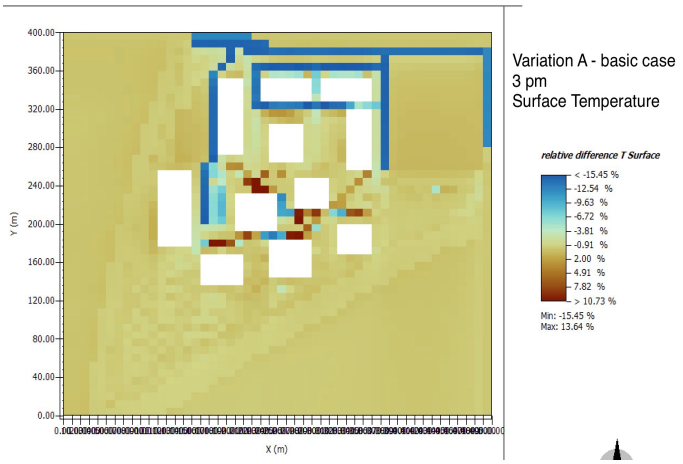

FIGURE 19 – ground delta surface temperature with basic at 3 pm

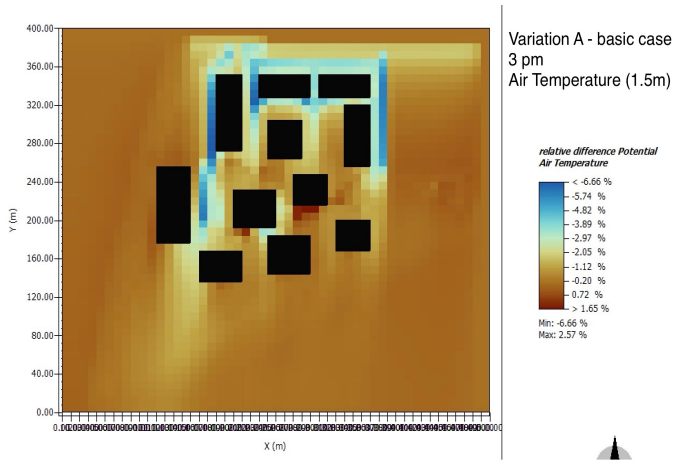

FIGURE 20 – ground delta air temperature with basic at 3 pm

3.3 Water body-environment interactions

3.3.1 Modifications and hypothesis

Excellent formulation of hypothesis and explanation of the reason linking to thermal behaviour of water, supported by numeric values.

In this part, we analyze the impact of water bodies on urban temperature variations. Water bodies are a critical tool for mitigating urban heat through evaporation, which absorbs heat and releases moisture into the atmosphere. Compared to asphalt, water has a significantly higher heat capacity (4186 J/(kg·K) vs. 920 J/(kg·K)), allowing it to store much more heat for the same temperature increase. This, combined with its lower surface temperature, makes water highly effective at regulating the urban thermal environment. Larger water bodies are particularly beneficial, as they provide a greater surface area for evaporation, enhancing their cooling potential.

To evaluate these effects, we designed two scenarios with an equal number of water squares in ENVI-MET to ensure a fair comparison. In both scenarios, water bodies were placed in sheltered locations to minimize wind effects. Excessive wind can disrupt cooling by increasing evaporation rates and carrying moisture away from the intended cooling area.

In the first scenario, we used irregularly shaped water bodies. While these shapes can result in localized cooling, their higher Length-Shape Index (LSI) reduces the uniformity of the cooling effect. These irregular forms were necessary to address ENVI-MET's limitations, which constrain the representation of non-rectangular shapes.

In the second scenario, we opted for more regular rectangular water bodies, strategically positioned between buildings and near heat sources such as a parking lot with elevated temperatures. These compact shapes, with lower LSI values, ensure better evaporative cooling and more uniform temperature distribution. Additionally, their placement near heat sources maximizes their localized cooling impact. The LSI of each water body is calculated using the formula :

$$LSI = \frac{D}{2\pi\sqrt{WA}} \tag{3}$$

where D is the perimeter and WA is the wetted area of the water body. The LSI values for the two configurations are given in the following table.

Scenario	LSI Value
Scenario 1 (Irregular Shape)	4
Scenario 2 (Regular Shape)	2

TABLE 4 – Length-Shape Index (LSI) for Each Scenario

Ideally, water bodies should be placed near vegetation rather than in narrow streets. Vegetation enhances cooling through evapotranspiration and benefits from the moisture provided by nearby water bodies, creating a synergistic effect. In contrast, placing water bodies in narrow streets limits airflow, reducing both cooling intensity and distance due to restricted urban ventilation. However, as this part of the study focuses on the independent effects of water bodies, the interaction between vegetation and water will be analyzed in the final case to provide a comprehensive evaluation.

By comparing these scenarios, we aim to understand how size, shape, and placement of water bodies influence their cooling performance, providing valuable insights for urban design strategies that optimize thermal comfort and mitigate the Urban Heat Island effect.

A graph should be provided to illustrate the geometry and location of the water body. What is the depth of the water body?

3.3.2 Results : Base case vs Regular configuration

After running the simulations, we generated the following graphs to analyze the results :

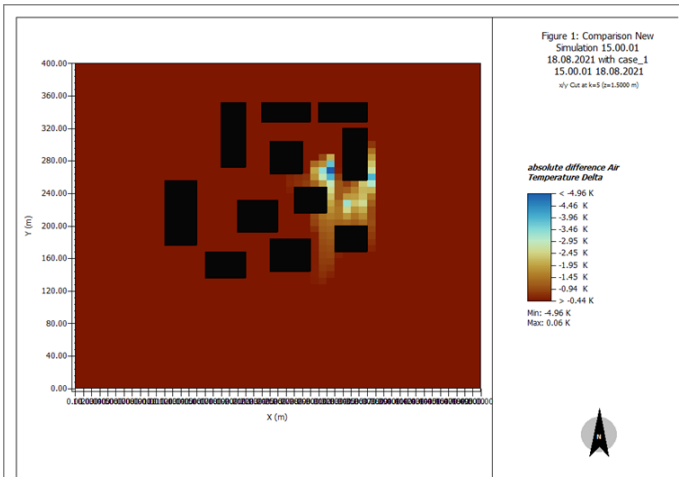

FIGURE 21 – Reduction in Air Temperature : Base Case vs. Regular Configuration

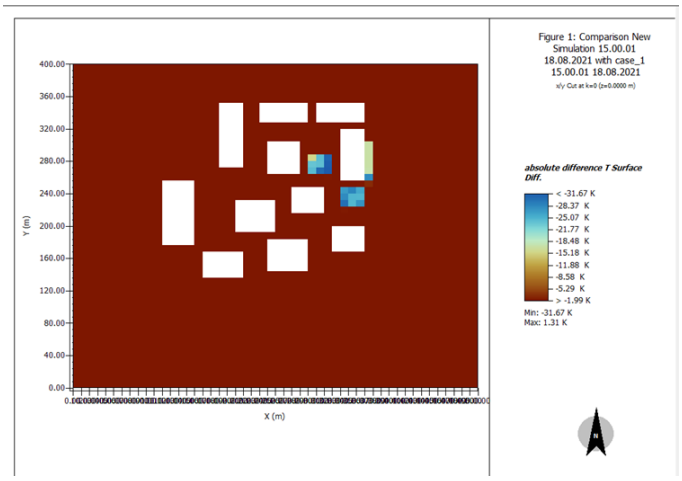

FIGURE 22 – Reduction in Surface Temperature : Base Case vs. Regular Configuration

Note : By "regular configuration," we refer to a regular shape configuration, and by "irregular configuration," an irregular shape configuration.The position of each water course is presented in the Appendix fig. 56 and 55.

The graph in Fig. 21 highlights the reduction in air temperature due to the presence of regular water bodies. Around x = 370, y = 280, the air temperature decreases by 2.5 K compared to the base case. This significant reduction demonstrates the efficiency of adding water in a sheltered area. By reducing wind exposure, these conditions enhance evaporative cooling, allowing the water bodies to regulate the surrounding air temperature more effectively and create a cooler microclimate.

The surface temperature graph (fig. 22) shows a decrease of 30 K near $x = 350, y = 240$, indicating strong local cooling. Regular water bodies reduce surface temperatures more effectively due to their larger contiguous areas, enhancing evaporation. The sheltered placement also contributes to reducing surface temperatures by maintaining stable evaporation rates. However, the narrow streets surrounding the water bodies may limit airflow and reduce the spread of the cooling effect.

3.3.3 Temperature difference : Regular vs Irregular configurations

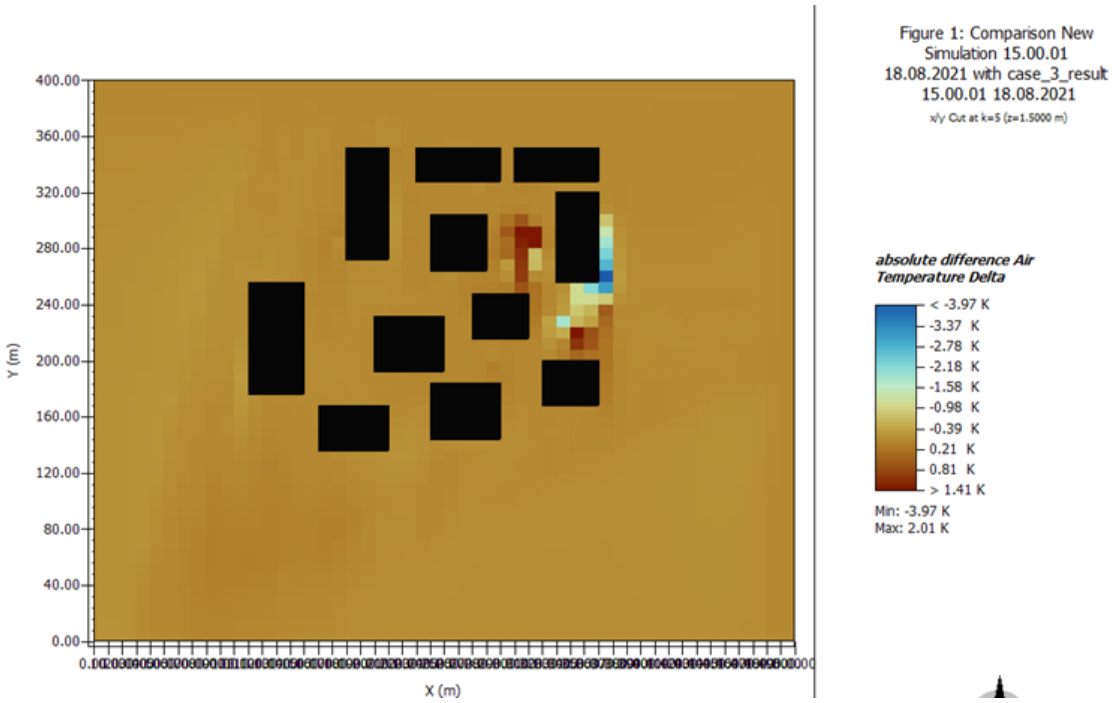

FIGURE 23 – Temperature Difference Between Regular and Irregular Configurations

As shown in fig. 23, direct comparison between the two scenarios suggests that irregular water bodies reduce air temperatures more effectively, with a reduction of up to 1.8 K more than regular shapes at $x = 310, y = 280$. This unexpected result might be attributed to ENVI-MET's limitations in accurately capturing the effects of irregular shapes, as the software represents surfaces as accumulations of squares, which could distort the representation of more complex geometries. Consequently, the performance of irregular shapes may be underestimated due to these constraints.

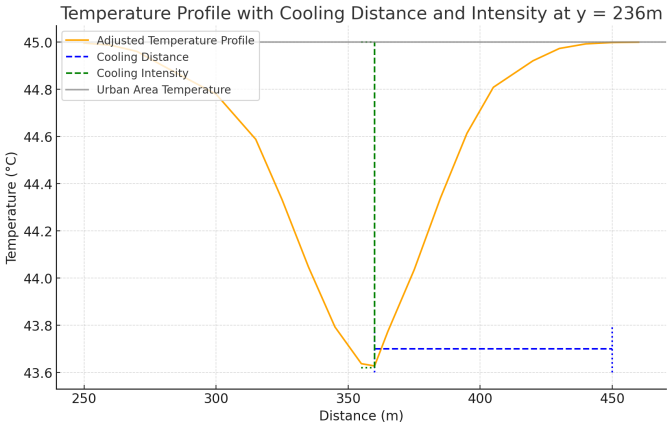

FIGURE 24 – Cooling Intensity for the Irregular Configuration

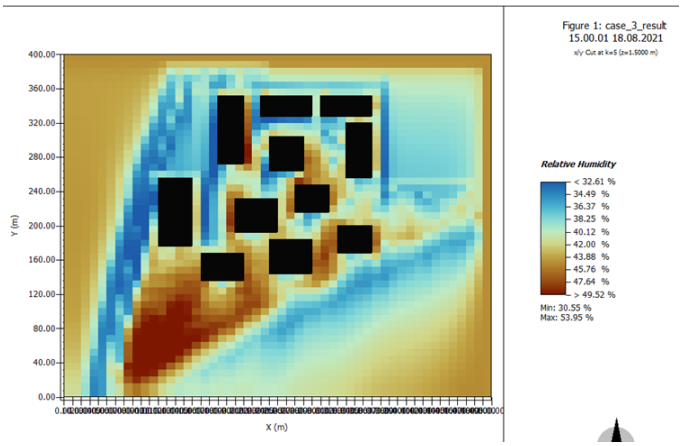

FIGURE 25 – Relative Humidity for the Irregular Configuration

3.3.4 Irregular case : Cooling Distance and Intensity

By exporting the data from "Leonardo" to Excel, we were able to calculate and plot the cooling distance and intensity for the irregular case with a single fixed water point at $y = 236$. This configuration is illustrated in Fig. 24, where the cooling distance and intensity vary across the defined x-range.
The graph highlights the following key observations :

- The cooling intensity reaches a maximum of 1.4 °C near $x = 360$, demonstrating the most effective cooling performance close to the water source. This is accompanied by a cooling distance extending up to 90 m, indicating significant influence in this zone.
- As we move further along the x-axis away from $x = 360$, both the intensity and distance gradually decrease, illustrating the diminishing cooling effect with increasing distance from the water point.
- Beyond $x = 450$, the cooling intensity levels off and the cooling effect becomes negligible. This reduction is not only due to the distance from the water point but also because of the presence of a building nearby, which obstructs the cooling influence.

This analysis emphasizes that the placement of the water point at $y = 236$ has a greatest impact on the cooling effect around $x = 360$. Why? Can you provide your explanation?

3.3.5 Final analysis

The results reveal, to our surprise, that irregular water bodies outperform regular ones in reducing air and surface temperatures, increasing humidity, and providing uniform cooling. For example, the 1.2 K reduction in air temperature near $x = 370, y = 280$ in the irregular scenario, although smaller than the 2.5 K reduction observed with regular shapes, demonstrated better resilience to wind disturbances due to a more diffuse distribution of evaporation zones. The more varied placement of irregular water bodies also seems to mitigate the constraints imposed by narrow streets, allowing slightly improved airflow and an expanded spatial reach of the cooling effect.

Future configurations should still prioritize integrating irregular water bodies with vegetation to create synergies between green and blue infrastructure. While the varied placement of these water bodies reduces wind disruption, balancing this feature with strategic positioning in well-ventilated areas could further amplify the cooling effects. This analysis confirms the unexpected advantage of irregular shapes, highlighting their potential for enhancing urban microclimate regulation.

3.4 Vegetation-environment interactions

In this part we want to see the effect of having vegetation in our zone. Urban vegetation is an important source of evaporation and shading. It contributes to the reduction of the heat urban islands effect and which really depends on the size of the green space, distribution and its composition. Urban

vegetation is a good strategy to mitigate the UHI effect because it has 2 major effects : reduction of the absorbed solar radiation by shading (radiative temperature decreases and improvement of outdoor thermal comfort) and increase the latent heat and take advantage of the evaporative cooling of air. We should observe a strong correlation between the surface temperature and the plant cover. If the trees are submitted to water shortage, then vegetation is useless for temperature reduction. The most effective plants for UHI mitigation are trees and that's why we are going to deal with them in this part.

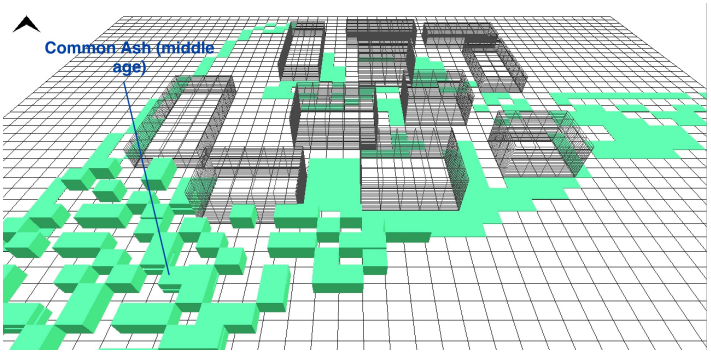

FIGURE 26 – Basic case vegetation

3.4.1 Modifications

In the first scenario, deciduous trees will be added to the maps. The species used are : Quercus Robur with a height of 25m and 15m crown width for the forest and Betula Pendula in parking with a height of 6m and crown width of 7m.

In the second scenario we will add evergreen plants. The species used are : picea abies for the forest and for parking cypress with a height of 15m and a crown width of 7m.

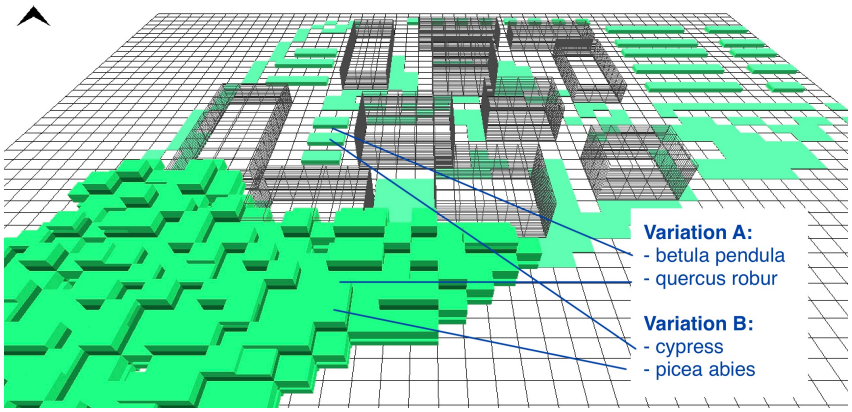

FIGURE 27 – Visualization of the modifications for both scenarios

3.4.2 Comparison of the two scenarios

The results of the simulation are the following :

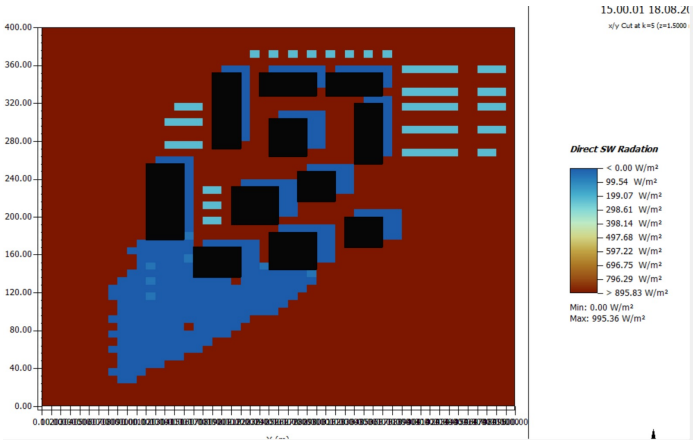

FIGURE 28 – Scenario 1 : Shortwave radiations

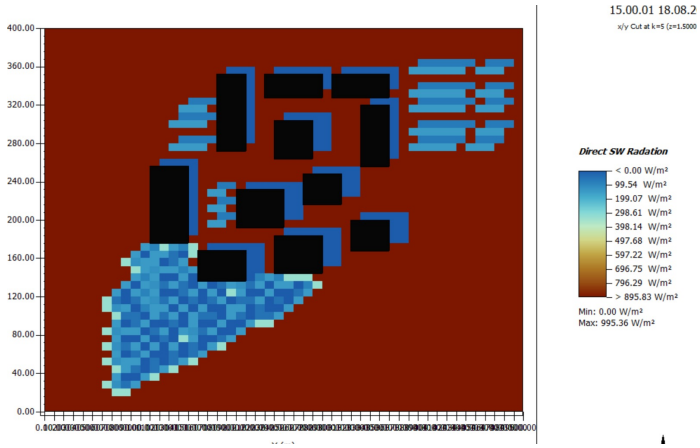

FIGURE 29 – Scenario 2 : Shortwave radiations

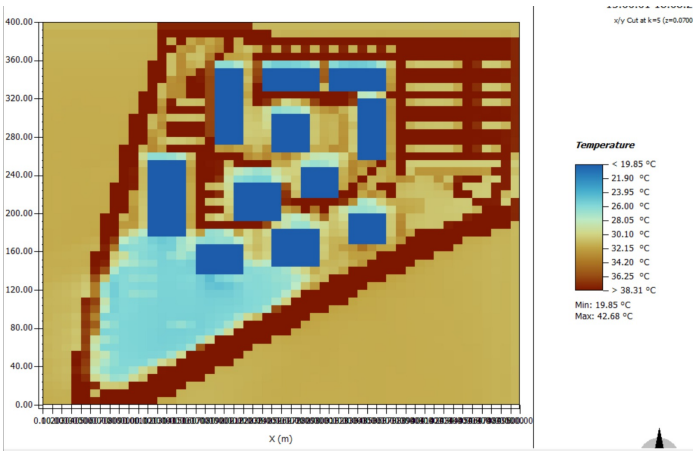

FIGURE 30 – Scenario 1 : Surface temperatures

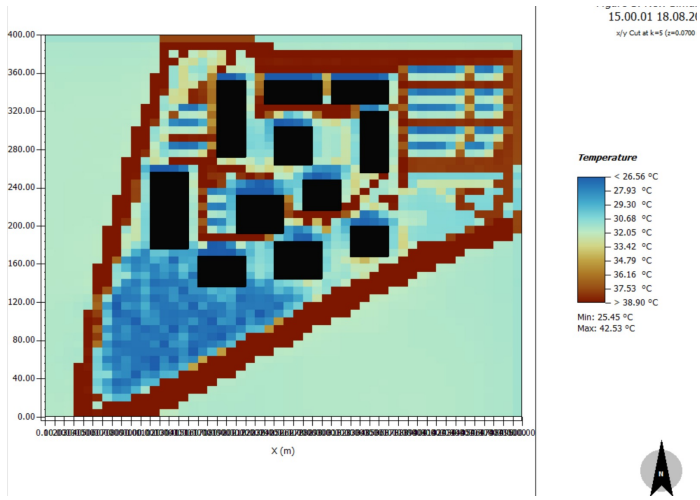

FIGURE 31 – Scenario 2 : Surface temperatures

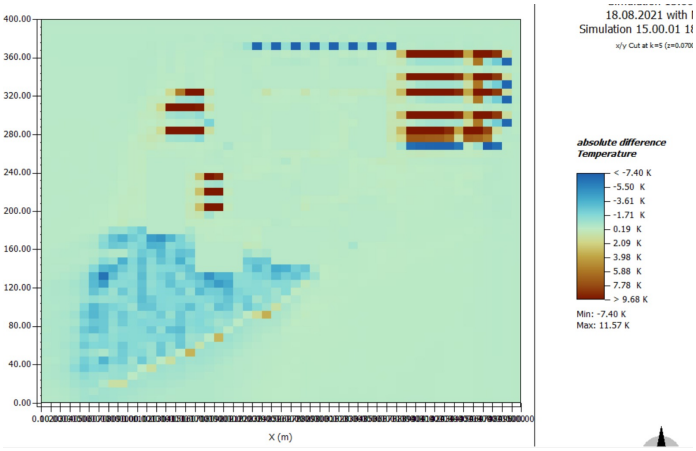

FIGURE 32 – Absolute difference for surface temperatures

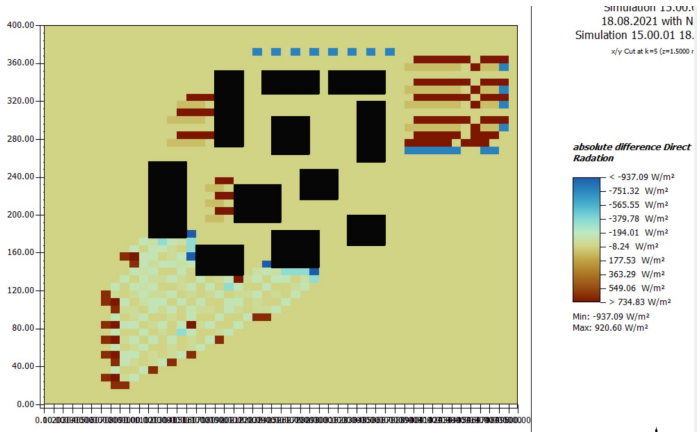

FIGURE 33 – Absolute difference for direct SW radiations

As said previously, the shading of the trees is very powerful for UHI mitigation. We can observe this on the shortwave radiations diagram for both scenarios. For both scenarios the direct SW radiations are almost reduced by a factor of 5 for some places where trees were added. The result of this is a significant reduction of the surface temperature around the trees. The canopy foliage attenuates the solar radiative flux by 70-90% in summer and 20-50% in winter for the deciduous trees and for the conifers it's more constant with a transmission of 10-30% year round.

The difference between your two scenarios in SW radiation can be linked to tree crown size and leaf area density.

One main difference between species of trees is that deciduous plants change their aspect with season, meanwhile the evergreen plants keep the same aspect. It can have an impact regarding the climate we have and according to the desired effect. Also, the wind speed can decrease up to 30% with trees because the vegetation is porous, and its aerodynamic effect is only a local effect.

Vegetation is also know for giving a good air quality which is an advantage for human comfort. A healthy mature tree in large canopy car sequester approximately 90 kg of carbon per year.

3.4.3 Comparison with the basic case

In this part the Figures 39 and 40 show the relative difference of air temperature for both scenarios with the basic case. It's a good way to see the results over the whole area and to find what is the best for each part.

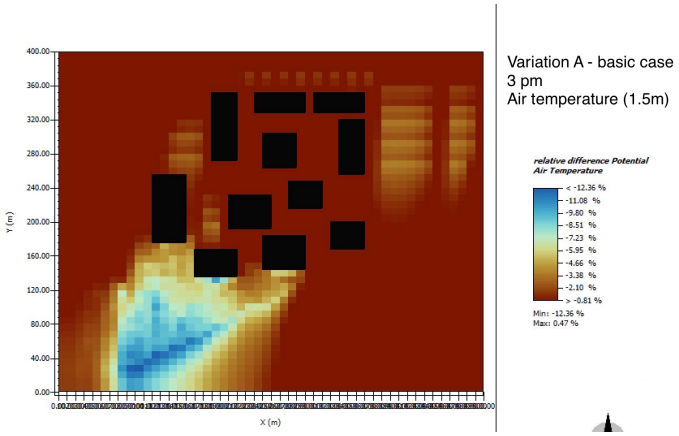

FIGURE 34 – Relative difference for air temperature Scenario 1 - Basic case

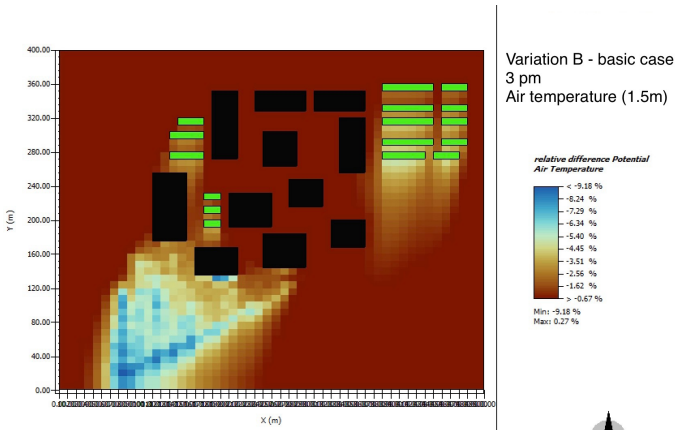

FIGURE 35 – Relative difference for air temperature Scenario 2 - Basic case

As a result we can observe that we need to add different species for parking and for forest. We can observe in the forest that the air temperature can decrease up to 12.36% with deciduous trees and up to 9.18% with picea abies. This is represented with a blue area on the pictures. The high density of the leaves for deciduous trees leads to more shading under the trees and then to lower temperatures. For the parking a lighter and larger area spreading to the South can be observed in the scenario 2. The form and density of the cypress is efficient because it doesn't stop the wind flux without variation during seasons. In comparison, the deciduous trees create a natural aeration under the canopy when they are all grouped together. It reinforces the reduction of temperature in the forest for example but when they are alone in a parking we can observe the opposite effect because the individual canopy will block the wind. We can also say that the positive effect of trees is very local but very efficient. We can observe this effect with blue or yellow zones on the maps which means that we have a pretty high difference in air temperature. The shading and evapotranspiration of the trees will improve the human outdoor comfort which is important point we need to take into account.

4 Integrated Microclimate Solution

What is the idea behind the final proposal?

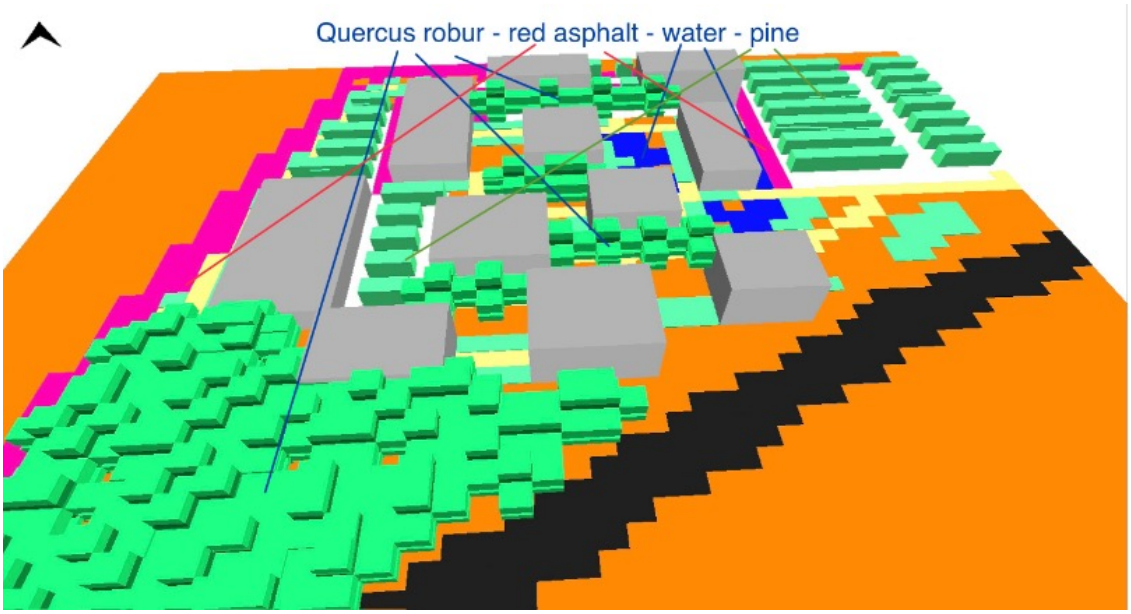

FIGURE 36 – Final case with modifications

4.1 Wind

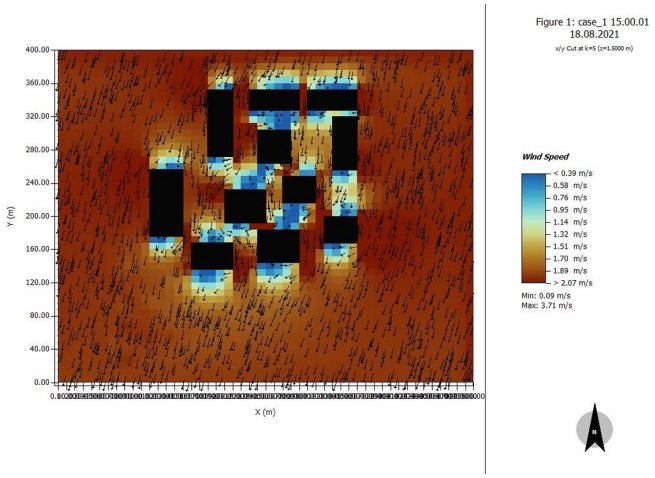

FIGURE 37 – Basic case

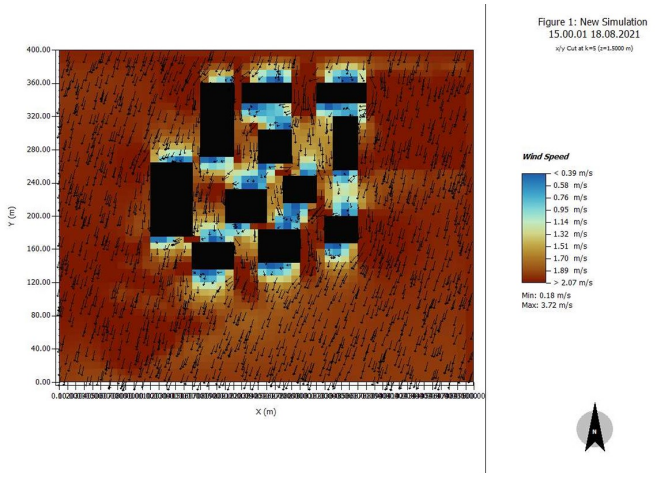

FIGURE 38 – Final case

As a result we can say that we don't really have an improvement with the wind as the scale of the wind speed and the colors of the maps are pretty similar. If we observe in detail, maybe we will observe small differences. In the middle of the building area we have a small reduction of the wind speed.

4.2 Temperatures

Why red, what is the albedo of red coating?

For the integrated solution, as shown in the ground section, a red coating was applied to the top and left sections of the asphalt, as it was the only ground modification that demonstrated a significant impact. The lower section, which is a high-traffic road, was not coated because the red coating would likely degrade quickly under heavy use. Although alternative coating colors, such as white, have been considered, the red coating was chosen because of its proven durability and established use over time. Experiments with coatings like white are ongoing, but current concerns about sunlight reflection and the loss of effectiveness as the surface becomes dirty led to the decision to favor the red coating for this scenario. The two figures below show the results we obtained for the surface temperature.

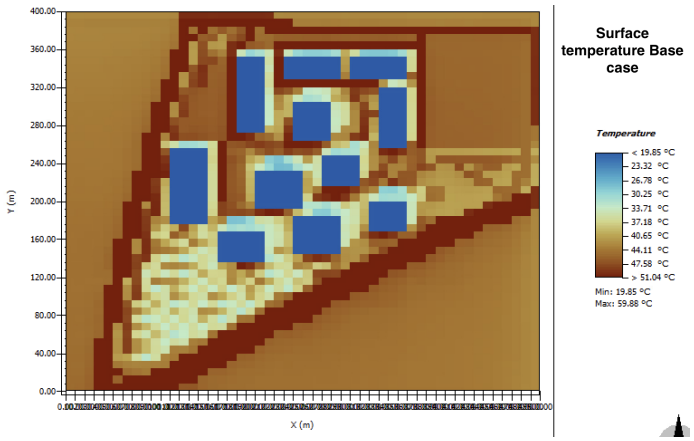

FIGURE 39 – Surface temperature basis case

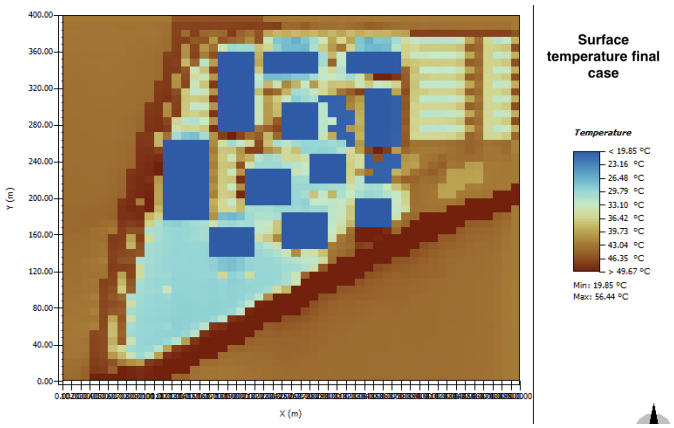

FIGURE 40 – Surface temperature final case

The wording 'lost' is not appropriate, try 'reduce' or 'decrease'

We observed a significant decrease in surface temperature, particularly on the asphalt where the red coating was applied, with temperatures dropping from 51°C to 40-45°C. Additional improvements resulted from the integration of trees and water. For example, in parking areas, we almost lost 10-15°C. In general, surface temperatures were reduced by 8 to 20°C in most areas. The site now maintains temperatures ranging between 20 and 40°C, which is much more acceptable compared to the baseline scenario.

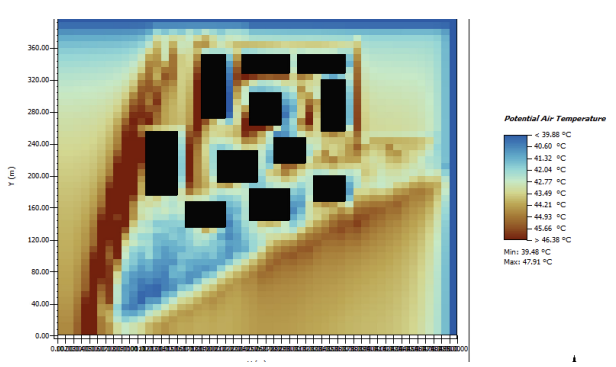

(a) Base case : Air temperature distribution.

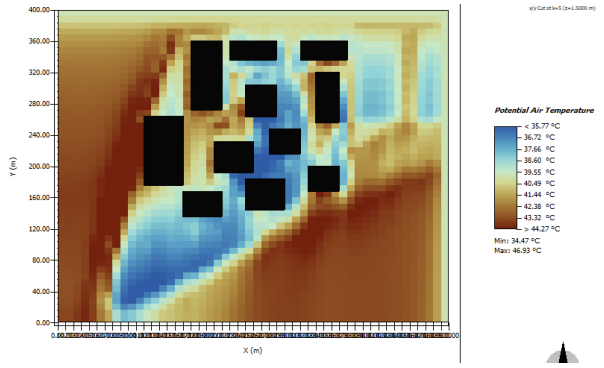

(b) Final case : Air temperature distribution.

FIGURE 41 – Comparison of potential air temperatures : Base case vs Final case.

In comparing the potential air temperature between the base case and the final case, the maps clearly illustrate a significant reduction in temperature in areas where water bodies were introduced in the final configuration. These reductions are particularly notable around the strategically placed water points, where the localized cooling effect is most pronounced. The high heat capacity and evaporative cooling properties of water have effectively decreased air temperatures in their immediate surroundings, as seen in the blue zones on the final case map.

This outcome validates our initial hypothesis regarding the role of water in mitigating urban heat. It demonstrates that, when water bodies are strategically located, they not only reduce localized temperatures but also contribute to a more comfortable urban microclimate. This highlights their critical importance as part of an integrated approach to urban heat mitigation.

4.3 Humidity

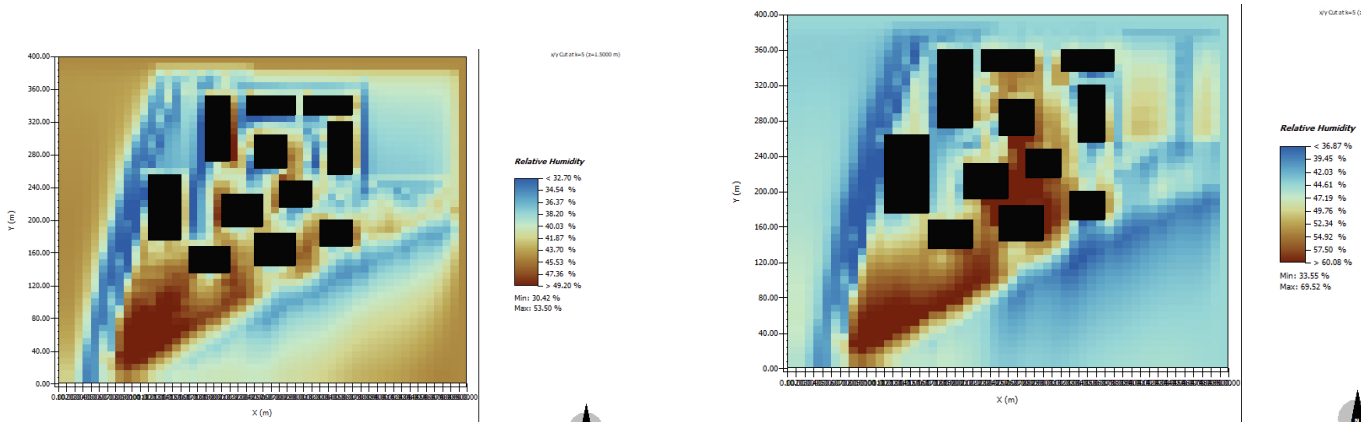

(a) Base case : Relative humidity.

(b) Final case : Relative humidity.

FIGURE 42 – Comparison of relative humidity between the base case and the final case.

To better appreciate the magnitude of the improvement in relative humidity (RH), it is crucial to focus on the numerical values rather than solely relying on the color gradients of the maps, as the visual representation may not fully reflect the extent of the changes. In comparing the base case and the final case, it is evident that the introduction of water bodies significantly enhances RH in the surrounding areas. While RH in the base case remains lower, particularly in zones dominated by impervious surfaces such as asphalt and concrete, the final case shows values ranging between 34 % and 65 %. This places the RH comfortably within the human comfort zone, which ranges between 30 % and 70 %.

4.4 Radiations

In this part we are going to analyze different graphs of shortwave radiations.

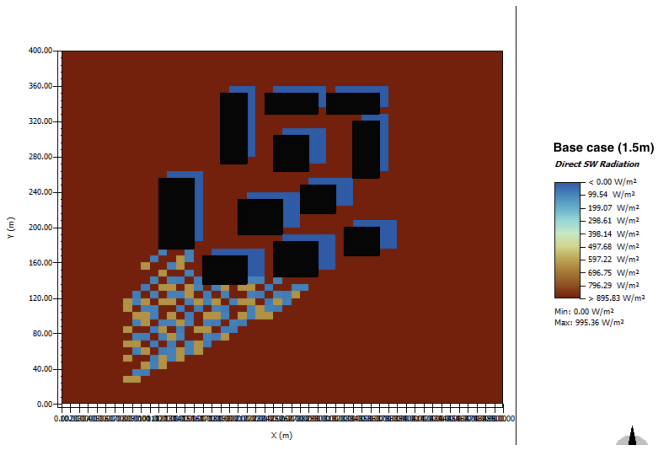

FIGURE 43 – Direct SW Radiation - Basic case

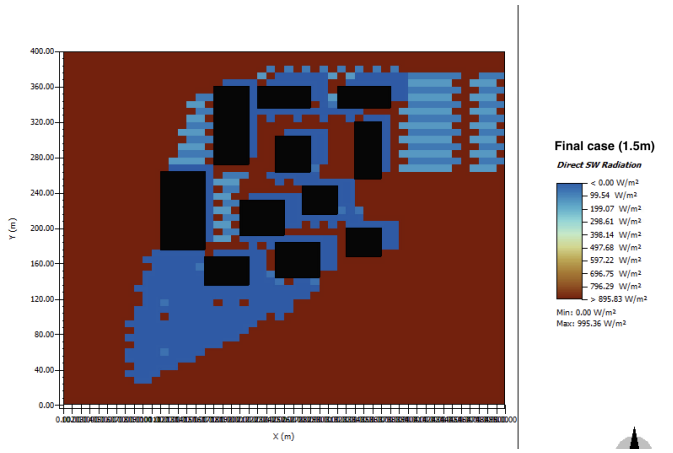

FIGURE 44 – Direct SW Radiation - Final case

The Figures 43 and 44 are showing the direct shortwave radiations. We can observe a huge difference mainly on the parking area where the intensity is much lower than on the basic case. This is due to the fact that the trees are providing shading. This leads to the reduction of the surface temperature and of the UHI. In the forest part, we almost have only a blue zone which the result of the shading of the trees. We can also observe a reduction of the shortwave radiations next to the building because they are also creating a shading zone.

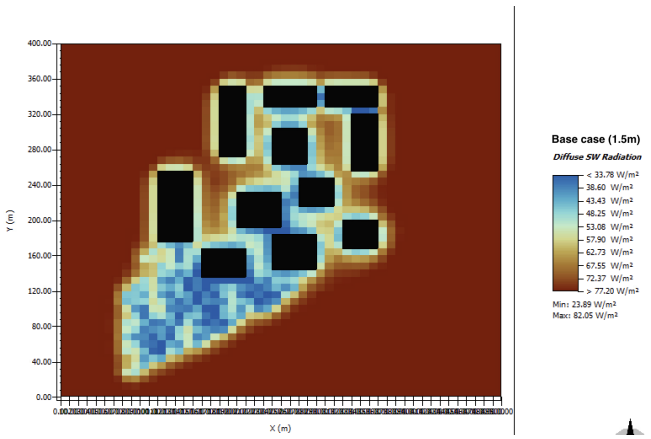

FIGURE 45 – Diffuse SW Radiation - Basic case

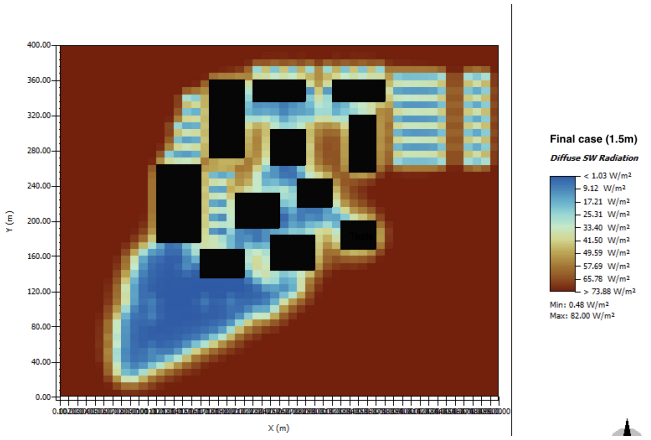

FIGURE 46 – Diffuse SW Radiation - Final case

The Figures 45 and 46 are showing the diffuse shortwave radiations. We can observe that we have smaller values between buildings or in the parking areas in the integrated solution. Buildings and trees are contributing to the reduction of the diffuse radiations.

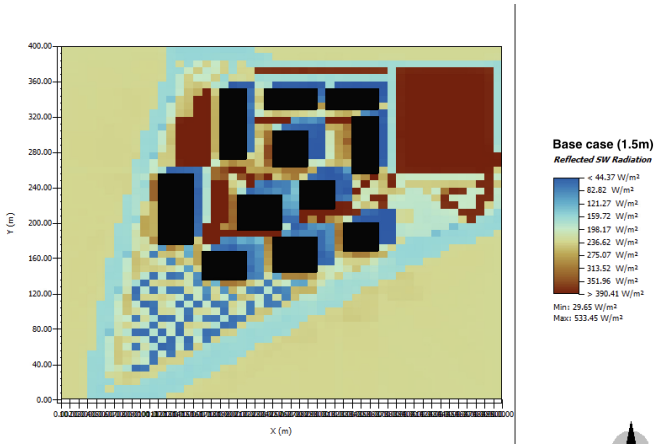

FIGURE 47 – Reflected SW Radiation - Basic case

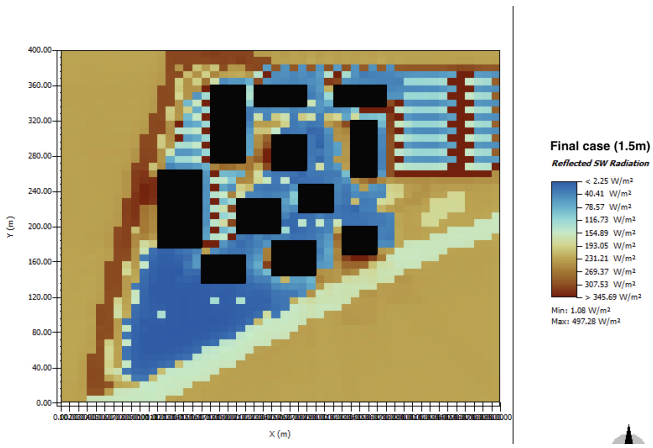

FIGURE 48 – Reflected SW Radiation - Final case

With these two graphs, we can observe the reflected shortwave radiations. We know that trees have a small albedo and we see it with blue areas next to the trees which means that they are not reflecting a lot of shortwave radiations. Buildings with their shadings are also reducing the amount that the surfaces can reflect.

4.5 Thermal Comfort Indices

4.5.1 Thermal comfort : PET

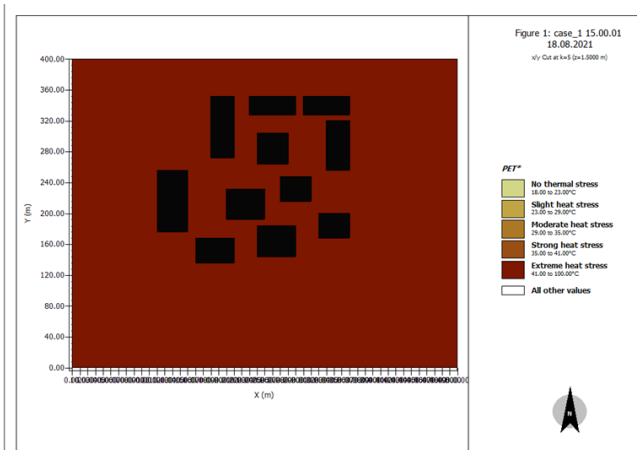

(a) PET : Basic case

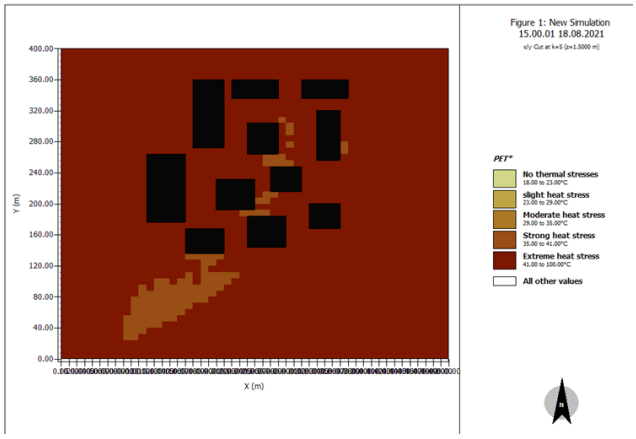

(b) PET : Best scenario

FIGURE 49 – Comparison between the optimal scenario and the baseline case for PET.

How was PET and UTCI calculate? What was the human parameters used?

The PET (Physiological Equivalent Temperature) highlights the differences in thermal comfort between the baseline and the optimal scenario. As shown on the maps, the optimal scenario significantly reduces perceived temperatures, particularly in densely vegetated areas or near water features. These improvements are attributed to the shading and evapotranspiration effects of trees, as well as the heat-absorbing capacity of vegetated surfaces and water bodies. However, certain dense urban areas show limited improvement, underscoring the limitations of PET in fully accounting for the complex interactions between buildings, wind, and radiation.

4.5.2 Thermal comfort : UTCI

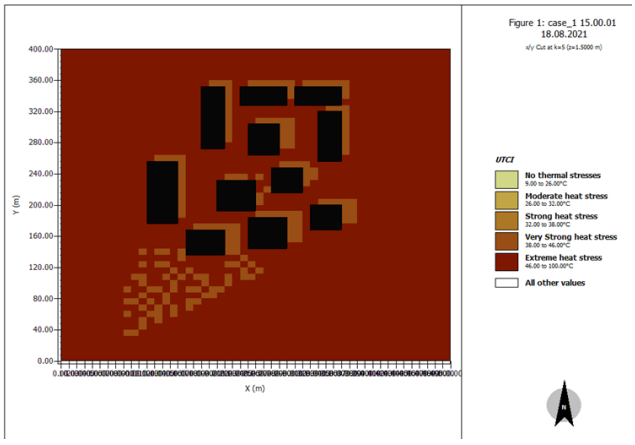

(a) UTCI : Basic case

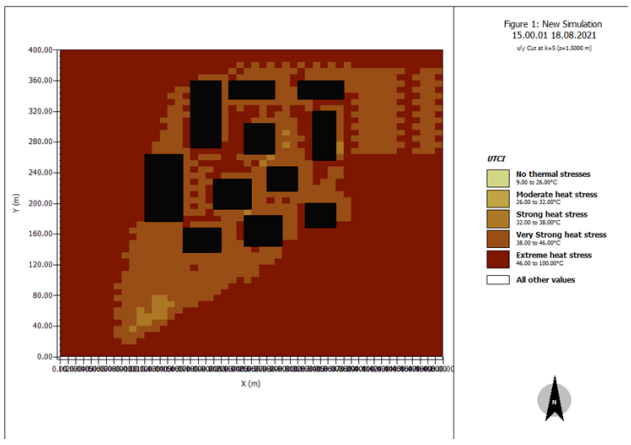

(b) UTCI : Best scenario

FIGURE 50 – Comparison between the optimal scenario and the baseline case for UTCI.

The optimal scenario, assessed using the UTCI (Universal Thermal Climate Index), demonstrates a more pronounced reduction in thermal stress compared to the baseline scenario. By incorporating dynamic factors such as wind and humidity, UTCI highlights the beneficial effects of wind corridors created by spaced buildings and shaded areas combined with water features. Unlike PET, UTCI also emphasizes the importance of open spaces in enhancing ventilation and dispersing heat. The improvements are particularly evident in areas with strong interactions between vegetation and water, where the microclimate becomes noticeably more comfortable.

Comparing the PET and UTCI results reveals that UTCI offers a more detailed and comprehensive evaluation of thermal conditions. While PET mainly emphasizes the direct effects of shading and materials, UTCI includes additional parameters, such as airflow dynamics, which significantly influence thermal comfort in urban environments. The optimal scenario is better captured by UTCI, as it more accurately reflects the benefits of interventions combining vegetation, water, and urban design. This complementarity makes UTCI more relevant to our study, especially for strategies aimed at reducing thermal stress in complex environments like the EPFL Innovation Park.

Both PET and UTCI take airflow into consideration.

4.6 Project Deepening and Limitations Related to Envi-MET

The ENVI-MET software proved invaluable in analyzing urban microclimate dynamics and testing mitigation strategies. However, several limitations must be acknowledged to contextualize the findings.

Firstly, the model relies on numerous assumptions and simplifications. For example, thermal properties of multi-layered materials were combined, and certain input parameters, such as emissivity, were estimated based on generic data. These approximations may reduce the precision of the results, especially for complex urban environments. Additionally, the limited spatial and vertical resolution of ENVI-MET can obscure fine details, such as narrow streets or small-scale vegetation, potentially underestimating localized effects.

Another significant limitation is the static nature of the simulations, which focus on specific time points rather than continuous dynamics. The cooling effects of water bodies and vegetation, which vary daily and seasonally, are thus only partially captured. Furthermore, the representation of irregular geometries, such as non-linear water bodies or intricate building designs, is constrained by the grid-based structure of the software, potentially underestimating their cooling potential.

While ENVI-MET excels in simulating natural processes such as air temperature, radiation, and evapotranspiration, it does not natively account for HVAC (Heating, Ventilation, and Air Conditioning) systems or their direct effects on the urban microclimate. However, users can input anthropogenic heat sources, including HVAC-related emissions, as external data to influence air temperature and wind patterns.

Finally, the computational demands of high-resolution simulations restricted the scale and number of scenarios analyzed. This limitation underscores the need for careful scenario selection and a balance between detail and feasibility to ensure meaningful insights without overloading computational resources.

Despite these constraints, ENVI-MET remains a powerful tool for exploring urban heat mitigation strategies. Future studies should integrate real-world data for calibration, complement ENVI-MET with field measurements, and consider parametric analyses to assess a wider range of conditions. While the findings of this project are indicative, they provide valuable insights for guiding urban planning and addressing the challenges of urban heat islands.

5 Conclusion

In conclusion, this project has provided a comprehensive exploration of urban overheating mitigation strategies for the EPFL Innovation Park, integrating analyses of microclimatic interactions and proposing targeted interventions to improve thermal comfort and sustainability. By leveraging ENVI-met simulations and combining theoretical insights with field observations, we have underscored the importance of holistic urban design in addressing the challenges posed by the Urban Heat Island (UHI) effect.

The findings reveal that effective mitigation requires a multifaceted approach. Vegetation emerged as a key element in reducing surface and air temperatures, with deciduous trees providing significant seasonal shading and evergreen species offering year-round benefits. Strategic placement of water bodies further amplified cooling through evaporation, while thoughtful modifications to building materials and ground surfaces enhanced thermal properties and reduced heat retention.

The integrated microclimate solutions proposed in this study demonstrate the potential to significantly reduce thermal stress in urban environments. For instance, the application of red coatings to asphalt surfaces, the inclusion of green walls and roofs, and the incorporation of reflective building materials proved effective in mitigating heat accumulation. Similarly, the alignment of wind corridors and the combination of vegetation with water features optimized airflow and evaporation, creating more comfortable and resilient urban spaces.

However, it is important to recognize the limitations of this study, particularly the constraints of the ENVI-met software in capturing dynamic and irregular urban elements. Future research should incorporate real-time data collection and higher-resolution simulations to refine the proposed strategies further. Moreover, a broader exploration of socio-economic factors and stakeholder engagement will be essential to ensure the feasibility and scalability of these interventions in diverse urban contexts.

Ultimately, this project reinforces the imperative of integrating climate-responsive design principles into urban planning. By prioritizing sustainability, human comfort, and environmental health, the proposed strategies for the EPFL Innovation Park serve as a model for other urban areas seeking to address the escalating challenges of climate change and urbanization. The insights gained here contribute to the growing body of knowledge on urban microclimates, paving the way for more adaptive and livable cities in the future.

6 Appendix

6.1 Table of construction materials

Category	Layer	Building Group A		Building Group B		Building Group C	
		Material	Thickness (m)	Material	Thickness (m)	Material	Thickness (m)
Façade	1	Prefabricated concrete wall	0.14	Plaster	0.01	Fiber cement board	0.008
	2	Insulation	0.1	EPS Expanded Polystyrene	0.18	Sandwich panel mineral wool	0.15
	3	Plaster	0.047	Plywood (heavyweight)	0.14	Aluminum	0.002
Roof	1	Gravel	0.05	Gravel	0.1	Gravel	0.04
	2	Insulation	0.2	XPS Extruded polystyrene CO2 blow	0.2	Mineral wool insulation	0.08
	3	Reinforced concrete slab	0.3	Concrete reinforced with 2% steel	0.3	Reinforced concrete slab	0.35
	4	--	--	EPS Expanded Polystyrene	0.065	--	--

FIGURE 51 – Table of construction materials for building groups A, B, and C.

6.2 Building group location

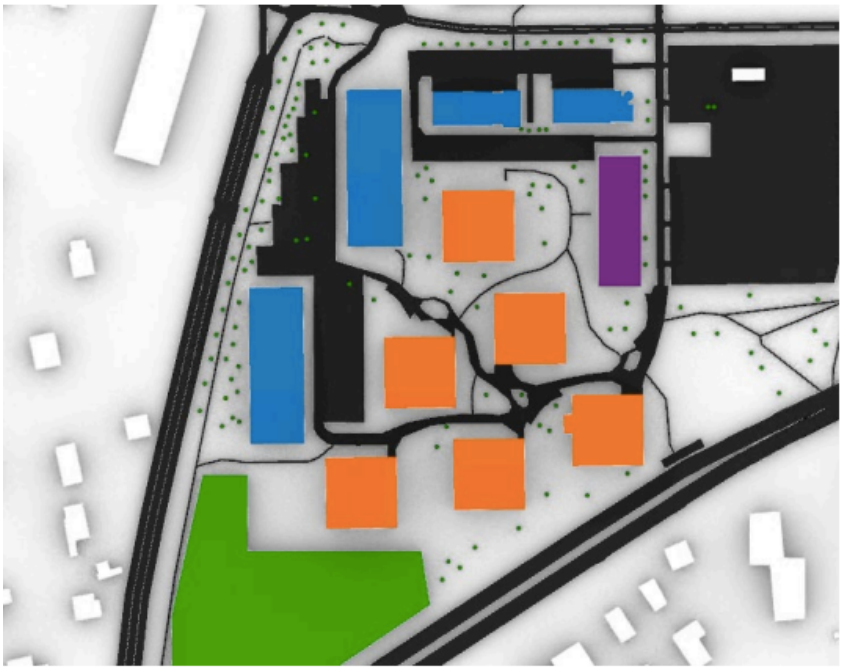

FIGURE 52 – Map showing the locations of Building Groups A, B, and C at the EPFL Innovation Park

6.3 Surface materials distribution map

FIGURE 53 – Map defining the materials for each area at the EPFL Innovation Park.

6.4 Thermal properties of the combined layers

Database-ID: [00000A]

Name: gravel+xps

Color:

Parameter	Value
Default Thickness	0.10000
Absorption	0.80000
Transmission	0.00000
Reflection	0.20000
Emissivity	0.90000
Specific Heat	1300.00000
Thermal Conductivity	0.20000
Density	757.00000
Extra ID	0

FIGURE 54 – Thermal and physical properties of the combined layers (Gravel + XPS).

6.5 Visualization of Water Body Positions for Regular and Irregular Configurations

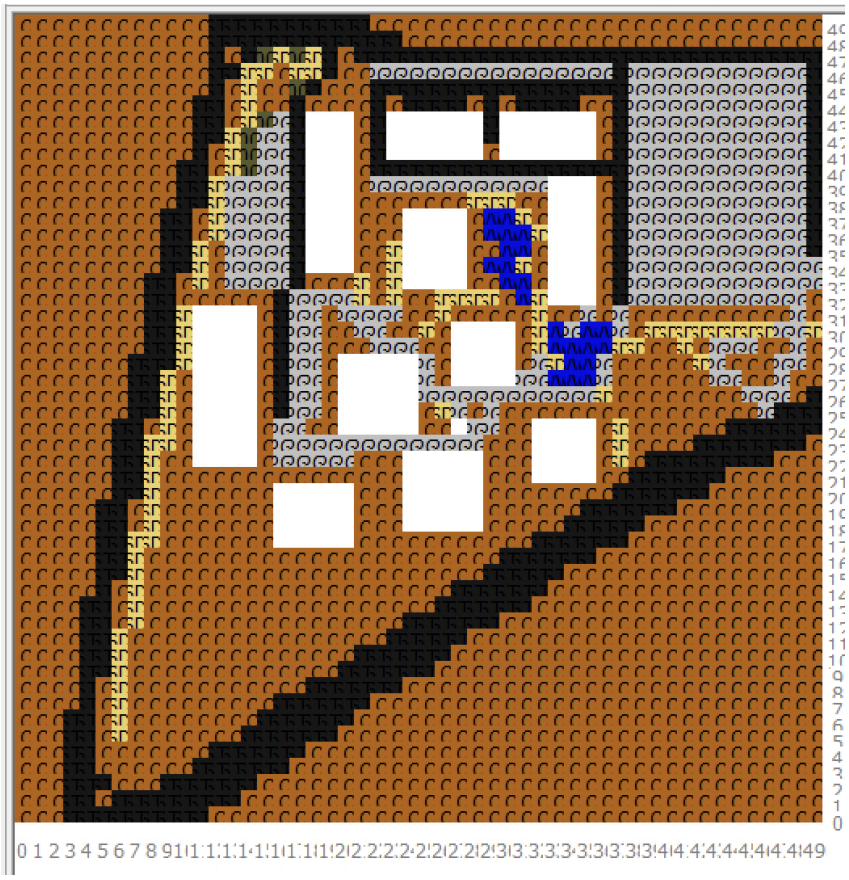

FIGURE 55 – Position of Water Bodies for the Irregular Configuration.

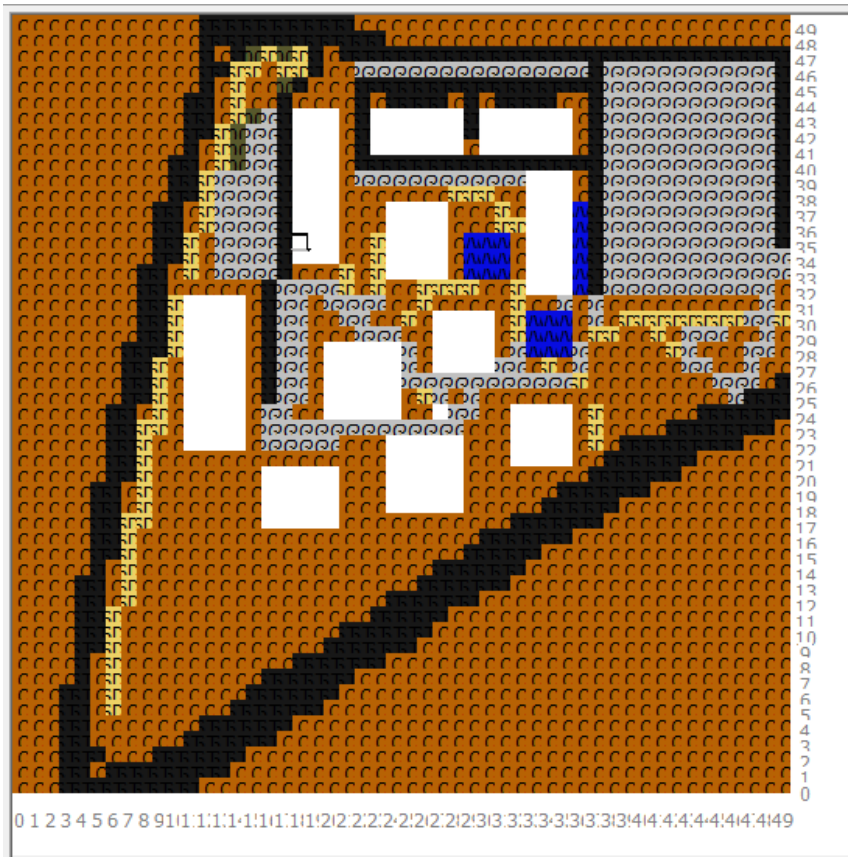

FIGURE 56 – Position of Water Bodies for the Regular Configuration.

7 References

[1] Logo EPFL :
https://inside.epfl.ch/corp-id/logo-fichiers/

[2] https://clima.cbe.berkeley.edu/